ELEMENTAL ANALYSIS OF GUNSHOT RESIDUE TO DIFFERENTIATE BULLET TYPE AND FIRING DISTANCE

By

Christine Ella Hay

A THESIS

Submitted to
Michigan State University
in partial fulfillment of the requirements
for the degree of

Forensic Science – Master of Science

2013

ABSTRACT

ELEMENTAL ANALYSIS OF GUNSHOT RESIDUE TO DIFFERENTIATE BULLET TYPE AND FIRING DISTANCE

By

Christine Ella Hay

Gunshot residue (GSR) was deposited on porcine tissue with hand loaded non-jacketed (NJ) and full-jacketed (FJ) ammunition at two different firing distances. Fresh tissue samples, as well as samples collected throughout decomposition were microwave digested in nitric acid and analyzed by inductively coupled plasma-optical emission spectroscopy (ICP-OES) and inductively coupled plasma-mass spectrometry (ICP-MS) to determine the elemental composition of the GSR. Element concentrations for lead (Pb), antimony (Sb), barium (Ba), copper (Cu), iron (Fe), and zinc (Zn) were statistically compared in order to investigate differentiation of bullet type and firing distance based on chemical concentrations in the GSR. Control (unshot) samples were collected in order to assess for environmental contaminants. Results of this study demonstrated that ICP-OES was adequate to detect the characteristic elements of GSR in fresh tissue, but was not sensitive enough to detect all elements throughout decomposition. Lead and Sb were significantly greater in NJ samples. Barium was useful in differentiating firing distance for both bullet types, while Cu was used to differentiate firing distance in FJ ammunition only. Analysis using ICP-MS, which has detection limits up to three orders of magnitude lower compared to ICP-OES, demonstrated the persistence of Pb, Sb, and Ba on porcine tissue throughout decomposition at a firing distance of 5 cm for both NJ and FJ ammunition.

ACKNOWLEDGMENTS

This work could not have been completed without the contributions of others. I would first like to acknowledge my advisor, Dr. Ruth Waddell Smith, for her guidance in the design, implementation, and completion of this project and thesis. I would also like to thank Dr. Ruth Waddell Smith, Dr. Brian Hunter, and Dr. Christopher Smith for serving on my thesis guidance committee. In addition, I would like to express thanks to Dr. Brian Hunter for his involvement with the design and implementation of the research.

I would like to acknowledge the following current and former MSU forensic chemistry students for their involvement with the completion of this research: Dr. Ruth Udey, John McIlroy, Emily Riddell, Andrew DeJarnette, and Joseph Stahl.

I would like to thank Dr. Kathy Severin from the MSU Chemistry Department and Justin Zyskowski from the Diagnostic Center for Population and Animal Health for access and guidance in the use of instrumentation. I would like to recognize the following MSU facilities, departments, and faculty for their contributions: Swine Teaching and Research Center (Al Snedgar and Kevin Turner), Dr. David Foran and former student Amanda Fazi from the Forensic Biology Program for access to a freezer, and Dr. Rich Merritt from the Entomology Department for permission to use their research field. I would like to show appreciation to the American Academy of Sciences Pathology/Biology Section and the Forensic Science Foundation Lucas Grant for providing funding to complete this research.

Finally, I would like to express thanks to my friends in the MSU Forensic Chemistry Program and the MSU Chemistry Department, my PhD advisor, Dr. Gary Blanchard, as well as my family for their support during my time at MSU.

TABLE OF CONTENTS

LIST OF TABLES

LIST OF FIGURES

Chapter 1: Introduction

1.1 Firearms and Ammunition

Firearms examination has been utilized in forensic science casework dating back to the early 20th century.[1] The types of physical evidence recovered in cases involving firearms include, but are not limited to, the firearm, shell casings, bullets, unused ammunition, and gunshot residue (GSR). The value of each type of evidence depends on the circumstances of the case. In early firearms cases, physical examinations of the firearm and ammunition were used to match the firing pin impressions or other physical impressions made on the bullet or casing. As advances in scientific methods and instrumentation have progressed, there is an increased value in identifying the chemical composition of evidence, for example, analyzing the elements present in GSR. In the event that a victim is found with a suspected gunshot wound, but no weapon or ammunition is recovered, confirming the presence of GSR may aid the police and medical examiner in confirming the cause of death. The ability to collect GSR evidence can be mitigated by the condition of the victim, in which case, sensitive analytical techniques are required to detect the chemical composition of small quantities of GSR.

Gunshot residue consists of burned and unburned particles of gunpowder, soot and/or vaporous lead, nitrite residues, and other particulate metals.[1] The GSR composition varies with the type of firearm and ammunition. Ammunition used in handguns, such as revolvers and pistols is composed of a cartridge case, primer, propellant, and a bullet or projectile (Fig 1.1). The cartridge case is a metal cylinder that houses the bullet, propellant, and primer in separate compartments. Cartridge cases are composed of metal alloys, such as brass or steel, where brass is a copper (Cu) and zinc (Zn) alloy and steel is an alloy composed primarily of iron (Fe).[2]

Figure 1.1 Non-jacketed (L) and full-jacketed (R) ammunition cartridges for a .357 revolver. For interpretation of the references to color in this and all other figures, the reader is referred to the electronic version of this thesis.

The primer, an explosive compound, is packed into the primer cup which is located at the base of the cartridge case. Common primers are composed of lead styphnate, antimony sulfide and barium nitrate which act as initiator, fuel, and oxidizer, respectively.[3] The combination of the primer metals, lead (Pb), antimony (Sb), and barium (Ba), in one GSR particle is characteristic of GSR.[4] The propellant is loaded into the cartridge case on top of the primer compartment, followed by the bullet. Propellants used in small firearms are typically smokeless powders that fall into two common classes. These classes are single-base and double-base smokeless powders. The primary component of single-base powders is nitrocellulose, while double-base powders contain nitrocellulose and nitroglycerin. Smokeless powders also contain compounds, such as stabilizers and plasticizers that vary in composition depending on the brand, but these compounds do not contain any metals of interest.

Bullets used in modern firearms fall into one of two categories, lead or metal-jacketed. Lead bullets, also known as non-jacketed (NJ) bullets, are primarily composed of lead, but may contain other metals, for example, antimony or tin to increase the hardness. Firing of a large number of lead bullets can cause a build-up of lead in the barrel of the firearm known as leading of the barrel. Metal-jacketed bullets have a thin layer of gilding metal, such as copper covering the lead core which prevents leading of the firearm barrel.[1] Metal jacketing of bullets can cover the lead core completely resulting in a full-metal jacket or full jacket (FJ).

The discharge of the weapon occurs when the firing pin strikes the primer cup. The primer is compressed between the primer cup and an anvil causing the primer to explode. Spheroid particles of GSR are formed as a result of the rapid heating in the primer cup and subsequent condensing of the vaporous metallic components of the primer.[1] The anvil, located

between the primer and the propellant, has vents that allow the flame to contact and ignite the propellant. The propellant deflagrates which causes an increase in the gas pressure inside the cartridge case. The cartridge case seals the chamber from release of gases until the build-up of pressure causes the bullet to be ejected from the cartridge and to move down the barrel of the firearm. Along with the bullet, a cloud of gas, soot, primer residue, and metallic components stripped from the bullet and cartridge case emerge from the barrel and are deposited as GSR on surfaces in the vicinity of the firearm.[2] Elemental contributions of commonly used primers (Pb, Sb, Ba) and cartridge cases (Cu, Zn, Fe) have been detected in GSR, while the contributions from the bullet depend on the bullet type. The elements found in primers can differ among brands and/or manufacturers and are therefore useful in differentiating ammunition.

1.2 SWGGUN and SWGGSR Guidelines

The Scientific Working Group for Firearms and Toolmarks (SWGGUN) has developed recommendations for procedures on the analysis of GSR evidence.[5] An updated set of guidelines for GSR firing distance determination was passed in November of 2011. According to the adopted guidelines, a microscopic examination of the victim's outer clothing should be followed by colorimetric tests including the modified Griess test, dithiooxamide (DTO) test, and the sodium rhodizonate test. The visible components of GSR, such as the unburned or partially burned gunpowder particles and the soot or vaporous lead deposits are visualized during the microscopic examination.

The colorimetric tests detect the presence of different chemical compounds or elements in GSR. The modified Griess test is used to detect the presence of nitrites, which originate from the propellant.[6] In this reaction, a positive test for nitrites results in the formation of a pink-violet

azo dye. This test needs to be conducted prior to other colorimetric tests to avoid chemical interferences. A positive DTO test results in the formation of colored precipitates in the presence of nickel (pink or blue), cobalt (brown), or copper (dark green), which is commonly found in GSR deposited with FJ ammunition.[7] The sodium rhodizonate test is indicative of the presence of vaporous lead, usually deposited at close range, and particulate lead residues originating from the bullet and/or firearm barrel.[8, 9] A bright pink color is observed in the presence of lead, while the presence barium can also be visualized when an orange color develops. Positive colormetric tests must be compared directly to negative controls with only reagent present in order to minimize the possibility of false positives. Colorimetric tests are specific for components of GSR; however, these tests are considered presumptive and further analysis is required to confirm the presence of GSR.

The Scientific Working Group for Gunshot Residue Analysis (SWGGSR) has published guidelines for the analysis of primer GSR by scanning electron microscopy with energy dispersive X-ray spectrometry (SEM/EDS), which will be described in more detail below, as well as a classification scheme for GSR.[4] Based on the elemental composition, a GSR particle is classified as 'characteristic', 'consistent with', or 'commonly associated' with GSR. A characteristic particle is said to contain element combinations that are not associated with other non-GSR particles. For example, a particle containing the three primer elements, Pb, Sb, and Ba, is considered characteristic of GSR when primers based on a so-called Sinoxid formulation are used. On the other hand, particles consistent with and commonly associated with GSR have elemental combinations that have been found in non-GSR sources, such as brake pads or fireworks. A particle containing Sb and Ba or Pb and Ba is consistent with GSR, while a particle

containing one of the three primer elements is commonly associated with GSR. Due to the focus on elemental composition of GSR, analytical techniques that are sensitive and specific for Pb, Sb, and Ba are useful in detection and classification of GSR. There is current research on the use of SEM/EDS, as well as other sensitive analytical instrumentation to detect GSR on clothing and skin tissue.

1.3 Current Research in Gunshot Residue Analysis

A standard technique for analyzing particulate components of GSR is SEM/EDS. Surveys of forensic science laboratories across the United States indicate that SEM/EDS has been widely used as a stand-alone method or in combination with a bulk analysis technique, such as atomic absorption spectroscopy (AAS).[10, 11] In 2010, the American Society for Testing and Materials (ASTM) updated their standard procedure for SEM/EDS analysis of GSR to be implemented in forensic science laboratories.[12] ASTM reported that SEM/EDS is advantageous to forensic scientists as it is non-destructive and provides both morphological and elemental information about GSR particles.

The SEM is capable of magnifying GSR particles that are typically one to five microns (10^{-6} m) in diameter more than 1000x in order to visualize the characteristic morphology.[13] The EDS provides X-ray analysis of the sample to determine the elemental composition of an individual particle. The combination of morphology and the presence of Pb, Sb, and Ba, in specified combinations, is a significant finding and is considered by some unique to the presence of GSR. The presence of two of the three elements is not considered unique to GSR as some combinations of Pb, Sb, and Ba have been recovered from non-firearm sources, such as brake pads and fireworks.[14-17] Environmental sources of GSR are continually studied in order to

strengthen the assertion that Pb, Sb, and Ba are only found together in GSR. One such study by Trimpe used SEM/EDS to analyze particles with morphology consistent with GSR recovered from burned fireworks.[18] A total of 148 fireworks were tested and of those, one primer metal (Pb, Sb, or Ba) was found in 117 of the residues, a combination of two primer elements was found in 18 of the residues, and no residues were found to contain all three elements in one particle. This study showed that the presence of the primer elements in non-GSR samples is not a rarity, but the presence of all three elements still provides confidence in the identification of GSR. Research utilizing SEM/EDS to detect GSR on shooter's hands and on other materials has positively identified GSR based on the presence of the Pb, Sb, and Ba under numerous experimental variations.[13, 19, 20]

Despite the obvious advantage of assessing particle morphology in combination with elemental composition, there have been some notable disadvantages of SEM/EDS reported.[21] The necessity of particle collection is a disadvantage especially in circumstances when the persistence of GSR particles is affected by environmental conditions and/or decomposition. In addition, the process of locating and testing particles under high magnification is time consuming when considering the size of the particles relative to the size of the adhesive tape used to collect the GSR.

Due in part to these limitations, other techniques for GSR analysis have been studied, such as AAS, inductively coupled plasma-optical emission spectroscopy (ICP-OES), and inductively coupled plasma-mass spectrometry (ICP-MS). These methods are bulk techniques that fail to provide morphological determinations; however, these are all analytical techniques that are utilized for their sensitivity in detecting the metallic components of GSR without the

need for collecting individual particles.[12] The bulk analytical techniques mentioned require samples of GSR to be dissolved or extracted prior to analysis and have been utilized on GSR collected from shooter's hands and other relevant materials. AAS has been used in combination with neutron activation analysis (NAA) in order to increase sensitivity for specific elements, such as Pb, Sb, and Cu.[22] NAA was utilized in particular for its sensitivity and specificity for Sb, but NAA is no longer widely applied since samples remain radioactive after analysis. Krishnan *et al*. found the utility of AAS was determined to be inadequate when detection of sub-part per million (mg/L) concentrations or detection of additional elements was desired. Koons *et al*. used ICP-OES instead of AAS to analyze Ba in solution extracts of GSR collection swabs.[23] The results showed ICP-OES achieved superior detection limits (<1 µg/L), had a wider dynamic linear range, and had fewer interferences from elements in the extract solution compared to AAS. In addition, ICP-OES was shown to be versatile since it is a multi-element analytical technique allowing for simultaneously analysis of many elements, whereas, AAS requires a separate analysis for each element of interest.

The choice of analytical technique for GSR depends on the desired sensitivity for different elements of interest. The most sensitive technique for Pb, Sb, and Ba currently used by forensic science researchers is ICP-MS. In 1998, Koons developed an ICP-MS method for detecting Pb, Sb, and Ba in GSR cotton swab extracts of shooter's hands.[24] In this work, the detection limits for Pb and Sb were an order of magnitude below those obtained using ICP-OES and the detection limit for Ba was improved by a factor of two for ICP-MS compared to ICP-OES. The improved detection limits for these three elements allowed for the determination of the persistence of GSR under real world conditions. LaGoo *et al*. developed a method for ICP-

MS elemental analysis of the persistence of GSR on porcine tissue.[21] In this study, GSR particles, as well as porcine tissue deposited with GSR were collected through a period of decomposition. Environmental factors affected the ability to collect GSR particles for SEM/EDS analysis beyond day 8 of decomposition, while the tissue samples were collected and analyzed by ICP-MS through 37 days of decomposition. The three characteristic elements of GSR were detected by ICP-MS on the porcine tissue throughout the decomposition study, whereas, only GSR particles collected on day 1 were found to be consistent with GSR using SEM/EDS.

The sensitivity of ICP-MS allows for the detection of elements in GSR that originate in the cartridge case or metal jacket, such as Cu, Fe, and Zn. These elements can aid in differentiation of ammunition and bullet type. Udey *et al*. utilized ICP-MS analysis on an expanded suite GSR elements, which are not all found in primers, including Cu, Fe, and Zn in order to differentiate FJ from NJ ammunition on shot porcine tissue.[25] The results of this study showed ICP-MS was adequately sensitive to detect all the elements of interest during moderate decomposition; however, Pb and Cu proved to be the most useful in differentiating bullet type. Wunnapuk *et al.* used ICP-OES for metal detection in acid digested skin tissue collected from fresh gunshot wounds.[26] In this study, ICP-OES proved to have adequate sensitivity for detection of Pb, Sb, Ba, as well as Cu, Fe, Zn and nickel (Ni). The elevated Pb concentrations in the fresh tissue shot with NJ ammunition were used to discriminate bullet type, while Fe and Zn were observed to have elevated concentrations in FJ samples.

In addition to differentiating bullet type, another practical application of GSR analysis is firing distance determination. Firing distance determinations were initially based on visual comparisons of GSR patterns and colorimetric tests for Pb and nitrites. A conventional method

for estimating firing distance was Walker's test, which involved imprinting the position of GSR particles from garments onto photo paper in order to compare with test firings.[27] Research utilizing analytical techniques to detect metals in GSR patterns of varying firing distances has focused on the quantification of one or two primer elements. Krishnan, as well as Gagliano-Candela *et al.* quantified Pb deposited in concentric circles around the bullet entrance hole by AAS.[28, 29] A linear relationship was found between the firing distance and the Pb concentration ($\log_{10}$) up to a firing distance of 100 cm. The higher sensitivity of ICP-MS analysis was utilized by Santos *et al*. for distance determination using Pb, Sb, and Ba.[30] ICP-MS analysis resulted in quantification of all three elements between firing distances of 20 and 80 cm with a linear relationship being established in this range Advancements in instrument sensitivity, precision, and accuracy of bulk analysis techniques make them useful in firing distance determination, but they have yet to be implemented in routine case work.

1.4 Research Objectives

The circumstances surrounding a homicide committed with a firearm vary greatly from case to case as does the amount of physical evidence to collect and process. The search for the most efficient and accurate method for GSR detection is ongoing. Cases involving decomposition of the victim can mitigate the quality and/or quantity of GSR evidence making it necessary to employ sensitive analytical techniques for analysis. Previous work has shown the detection of characteristic elements of GSR, as well as elements used to differentiate bullet type by ICP-MS.[25] ICP-MS is a sensitive elemental analysis technique; however, it is not widely available in forensic science laboratories and the cost per analysis can be expensive. A more accessible and inexpensive elemental analysis technique would be useful as long as adequate

sensitivity for the elements of interest can be attained. As demonstrated by Wunnapuk *et al.*, ICP-OES is adequate to detect GSR in shot tissue; however, this technique has not been used to detect GSR in decomposed tissue samples.[26]

The objective of this research was to develop an ICP-OES procedure for the elemental analysis of GSR on porcine tissue. The results were compared to ICP-MS results to evaluate the utility of both techniques in GSR detection. GSR analysis of the porcine tissue shot while varying bullet type and firing distance was completed through decomposition. Ammunition with NJ bullets was used to deposit GSR onto porcine tissue at firing distances of 5 and 10 cm. Those firing distances were also used for GSR deposition with FJ ammunition. In fresh tissue samples, the ability to detect GSR elements from different bullet types at two firing distances was determined and the elemental concentrations were compared in order to differentiate bullet type. Differentiation of firing distance was assessed for tissue samples shot with the two different bullet types. The same comparisons were made for the tissue samples collected throughout decomposition, and the persistence of GSR on the shot tissue was assessed.

REFERENCES

REFERENCES

1. Heard BJ. Handbook of firearms and ballistics. 2nd ed. Chichester, West Sussex, UK: John Wiley & Sons, Ltd, 2008.

2. DiMaio VJM. Gunshot wounds: Practical aspects of firearms, ballistics, and forensic techniques. 2nd ed. Boca Raton: CRC Press, 1999.

3. Schwoeble AJ, Exline DL. Current methods in forensic gunshot residue analysis. Boca Raton, FL: CRC Press; 2000.

4. SWGGSR. Guide for primer gunshot residue analysis by scanning electron microscopy/energy dispersive x-ray spectrometry 2011.

5. ASCLD/LAB-International. Supplemental requirements for the accreditation of forensic science testing laboratories; ISO:17025, 2006.

6. Steinberg M, Leist Y, Goldschmidt P, Tassa M. Spectrophotometric determination of nitrites in gunpowder residue on shooters hands. J Forensic Sci. 1984; 29:464-70.

7. Lekstrom JA, Koons RD. Copper and nickel detection on gunshot targets by dithiooxamide test. J Forensic Sci. 1986; 31:1283-91.

8. Harrison HC, Gilroy R. Firearms discharge residues. J Forensic Sci. 1959; 4:184-99.

9. Bartsch MR, Kobus HJ, Wainwright KP. An update on the use of the sodium rhodizonate test for the detection of lead originating from firearm discharges. J Forensic Sci. 1996; 41:1046-51.

10. DeGaetano D, Siegel JA. Survey of gunshot residue analysis in forensic science laboratories. J Forensic Sci. 1990; 35:1087-95.

11. Singer RL, Davis D, Houck MM. A survey of gunshot residue analysis methods. J Forensic Sci. 1996; 41:195-8.

12. ASTM Standard E1588, 2010, Standard guide for gunshot residue analysis by scanning electron microscopy/energy dispersive x-ray spectrometry, ASTM International, West Conshohocken, PA, 2010, DOI: 10.1520/E1588-10e01, www.astm.org

13. Andrasko J, Maehly AC. Detection of gunshot residues on hands by scanning electron microscopy. J Forensic Sci. 1977; 22:279-87.

14. Torre C, Mattutino G, Vasino V, Robino C. Brake linings: A source of non-gsr particles containing lead, barium, and antimony. J Forensic Sci. 2002; 47:494-504.

15. Grima M, Butler M, Hanson R, Mohameden A. Firework displays as sources of particles similar to gunshot residue. Sci Justice. 2012; 52:49-57.

16. Mosher PV, McVicar MJ, Randall ED, Sild EH. Gunshot residue-similar particles produced by fireworks. Can Soc Forensic Sci J. 1998; 31:157-68.

17. Trimpe MA. The current status of gsr examinations. FBI Law Enforcement Bulletin; May 2011.

18. Trimpe MA. Analysis of fireworks for particles of the type found in primer residue (gsr). International Association for Microanalysis Newsletter; 2003;1-7.

19. Wolten GM, Nesbitt RS, Calloway AR, Loper GL, Jones PF. Particle analysis for the detection of gunshot residue. I: Scanning electron microscopy energy dispersive-x-ray characterization of hand deposits from firing. J Forensic Sci. 1979; 24:409-22.

20. DeGaetano D, Siegel JA, Klomparens KL. Comparison of three techniques developed for sampling and analysis of gunshot residue by scanning electron microscopy/energy dispersive x-ray analysis. J Forensic Sci. 1992; 37:281-300.

21. LaGoo L, Schaeffer LS, Szymanski DW, Smith RW. Detection of gunshot residue in blowfly larvae and decomposing porcine tissue using inductively coupled plasma mass spectrometry (icp-ms). J Forensic Sci. 2010; 55:624-32.

22. Krishnan SS, Gillespie KA, Anderson EJ. Rapid detection of firearm discharge residues by atomic absorption and neutron activation analysis. J Forensic Sci. 1971; 16:144-51.

23. Koons RD, Havekost DG, Peters CA. Determination of barium in gunshot residue collection swabs using inductively coupled plasma-atomic emission-spectrometry. J Forensic Sci. 1988; 33:35-41.

24. Koons RD. Analysis of gunshot primer residue collection swabs by inductively coupled plasma-mass spectrometry. J Forensic Sci. 1998; 43:748-54.

25. Udey RN, Hunter BC, Smith RW. Differentiation of bullet type based on the analysis of gunshot residue using inductively coupled plasma mass spectrometry. J Forensic Sci. 2011; 56:1268-76.

26. Wunnapuk K, Durongkadech P, Minami T, Ruangyuttikarn W, Tohno S, Vichairat K, et al. Differences in the element contents between gunshot entry wounds with full-jacketed bullet and lead bullet. Biol Trace Elem Res. 2007; 120:74-81.

27. Walker JT. Chemistry and legal medicine. New Engl J Med. 1937; 216:1024-7.

28. Krishnan SS. Firing distance determination by atomic absorption spectrophotometry. J Forensic Sci. 1974; 19:351-6.

29. Gagliano-Candela R, Colucci AP, Napoli S. Determination of firing distance. Lead analysis on the target by atomic absorption spectroscopy (aas). J Forensic Sci. 2008; 53:321-4.

30. Santos A, Magalhaes T, Vieira DN, Almeida AA, Sousa AV. Firing distance estimation through the analysis of the gunshot residue deposit pattern around the bullet entrance hole by inductively coupled plasma-mass spectrometry - an experimental study. Am J Foren Med Path. 2007; 28:24-30.

Chapter 2: Theory

2.1 Microwave-Assisted Digestion

Microwave-assisted digestion procedures for sample preparation have replaced techniques, such as wet digestion, dry ashing, and fusion.[1] Microwave digestion is superior to these techniques in terms of reduced contamination, increased safety, decreased amounts of sample and reagents, as well as the applicability to a large number of biological and environmental sample matrices.

Prior to elemental analysis, solid samples must be converted into a liquid form. The chosen digestion process must completely break down the sample matrix until the analytes of interest are solubilized. In microwave-assisted digestion, solid samples are immersed in reagents to aid in solubilization and then heated in a microwave oven. The development of microwave heating techniques started in the 1940s.[2] Since microwave radiation falls at the low energy end of the electromagnetic spectrum (10^{-5}–10^{-2} eV), it is non-ionizing and interacts with matter at the molecular level.[2]

The heating properties of microwaves rely on the ability of a substance to absorb microwave radiation and convert this energy to heat. Dipole rotation and ionic conduction are two phenomena required for microwave heating. For dipole rotation to occur, the dipole of a molecule aligns with the electric field that is applied upon microwave irradiation. The molecular movement in response to the dipole alignment generates thermal energy. Ionic conduction also results in generation of heat, but occurs as a result of movement of ions. When a solution of ions experiences an applied microwave electromagnetic field, the positive and negative ions migrate

to opposite poles. As the ions migrate across the induced gradient, ions experience resistance from solvent molecules, which results in heat generation.

Microwave ovens have been used as a heating source for digestion processes since the 1970s.[3] Household microwave ovens were initially used for heating samples; however, modifications allowing for control over temperature ramps and constant power output have been made to enhance the digestion process. For digestion of biological samples, a closed vessel set-up in a cavity oven is preferred.[2] A cavity oven implies a multimode operation in which microwave radiation is dispersed into a large cavity as opposed to focused on one sample. This type of oven allows for multiple samples to be digested simultaneously while the closed vessel set-up is conducive to a fast digestion time. As digestion of the sample progresses, the decomposition of the sample and the evaporation of the solvent molecules cause the gas pressure in the closed vessel to increase. This increased pressure in the vessel results in an increase in the boiling point of the solution, thereby, aiding in the oxidant power of reagents, such as nitric acid, and shortening the digestion time.

The reagents used for digestion are not defined specifically for all tissue or other biological samples; however, the combination of an acid, such as nitric acid, and an oxidizing agent, such as hydrogen peroxide, is well-documented.[4] Nitric acid is a strong acid that does not form insoluble products making it compatible with a number of biological samples and analytical techniques. Hydrogen peroxide is commonly used as an oxidant to enhance the complete decomposition and solubilization of the sample.

2.2 Inductively Coupled Plasma-Optical Emission Spectroscopy

Inductively coupled plasma-optical emission spectroscopy (ICP-OES) is an elemental analysis technique capable of measuring sub-part per million (mg/L) element concentrations. This technique is routinely used to detect and quantify elements in biological and environmental samples by recording the line spectra of elements of interest as radiation is emitted. ICP-OES analysis can provide precise and accurate wavelength identification over a wide linear range.[5]

ICP-OES is primarily used to analyze the elemental composition of liquid samples. Sample introduction is a multistep process, which begins with pumping the sample liquid through a peristaltic pump into a nebulizer.[6] The peristaltic pump is equipped with rollers that move at the same rate to ensure a continuous flow of liquid samples and blanks. In the nebulizer, the liquid samples are broken up into fine aerosol made up of small liquid droplets by a high velocity flow of gaseous argon (~1 L/min). The droplet selection process takes place in the spray chamber. The fine droplets in the aerosol enter the spray chamber, where small droplets (~5–10 μm in diameter) traverse the length of the spray chamber's central tube, while the larger droplets fall out of the aerosol into the outer tube of the spray chamber due to gravity. The fine droplets are carried into the plasma torch via the sample injector for desolvation, atomization, and ionization.

The plasma torch is composed of three concentric quartz tubes, the outer tube, the middle tube, and the sample injector. A cross-sectional view of a plasma torch with labeled heating zones is shown in Figure 2.1. The outer quartz tube is surrounded by an induction coil that is powered by a radio frequency (RF) generator. An alternating current in the coil matching the frequency of the generator produces a fluctuating magnetic field. A source of argon gas flowing at approximately 1 L/min is directed between the outer and middle quartz tubes.[7]

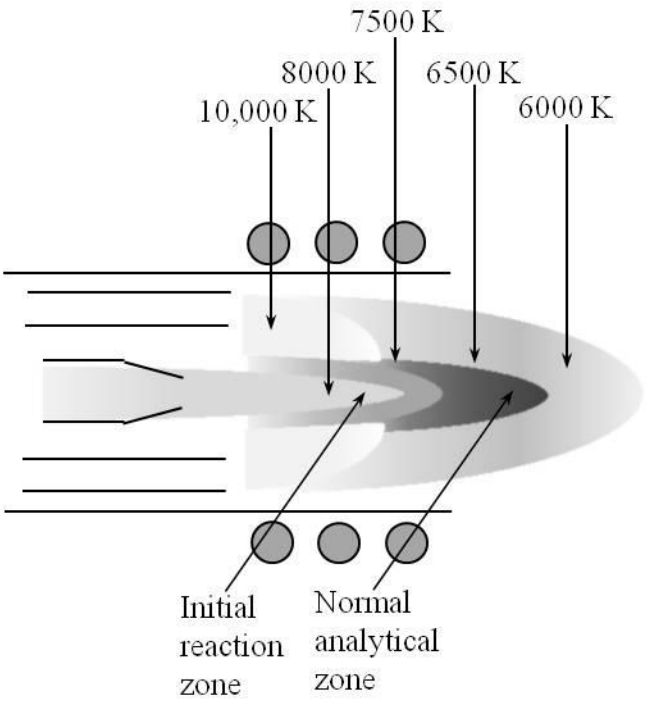

Figure 2.1 Inductively coupled plasma torch heating zones. Adapted from Thomas (2001).[7]

A high voltage spark initiates ionization of the argon gas. The resulting argon ions and electrons interact with the magnetic field and flow in closed annular paths. The resistance of the ions and electrons to flow causes Ohmic heating in the plasma torch. The plasma torch is maintained at a temperature of approximately 10,000 K in the core surrounded by the induction coil.[5] A second stream of argon, the auxiliary gas, flows between the middle quartz tube and the sample injector in order to center the plasma and thermally isolate the quartz cylinder. The third gas flow is the nebulizer flow of argon that carries the fine aerosol sample into the center of the plasma. As the aerosol sample moves through different heating zones within the plasma, the droplets are desolvated to produce a solid sample. The solid is vaporized to its gaseous form and then atomized forming a ground state atom.[8] Ions are also formed in the plasma when argon ions and electrons collide with ground state atoms resulting in the removal of an outer electron.

A fraction of the sample atoms and ions are thermally excited in the heat of the plasma. The lifetime of the excited state is very short before radiation of a specific wavelength is emitted. Spectral observations are recorded in an optically transparent region beyond the induction coil where the temperature is in the range of 6000 to 6500 K.[5] The emitted radiation is directed into a spectrometer that selects and detects the wavelengths emitted as shown in Figure 2.2. The most commonly used spectrometer type is a simultaneous multichannel instrument with a solid state array detector, such as a charge coupled device. This type of OES instrument utilizes an optical grating to spatially separate the emission wavelengths and then measures all of the wavelengths simultaneously. An emission spectrum of intensity as a function of wavelength is recorded for each element and the intensity corresponding to wavelength of maximum emission is used to determine the element concentration relative to a standard calibration curve.

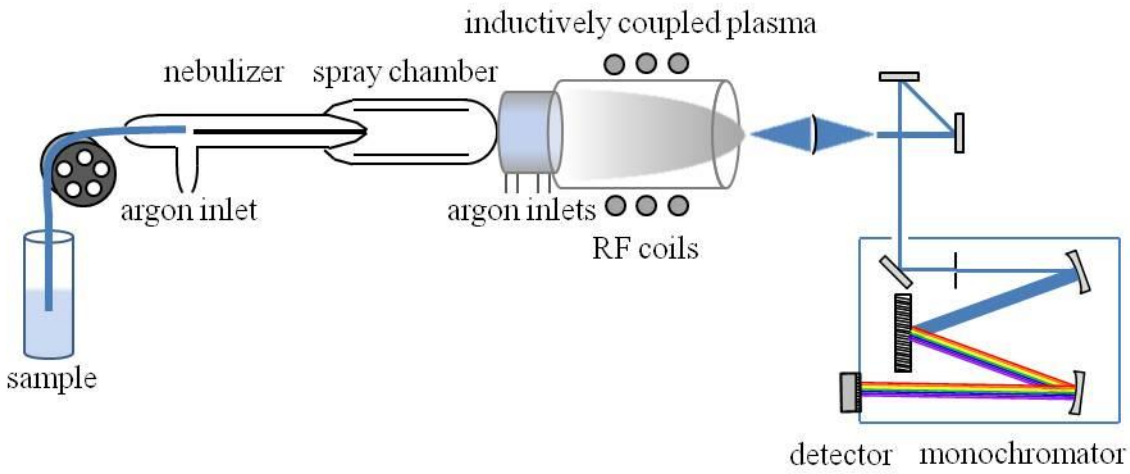

Figure 2.2 Schematic of inductively coupled plasma-optical emission spectrometer.

The emission lines of each element correspond to energy differences in the electron orbitals. These electronic transitions are well defined for most elements; however, only about 60 elements have emission lines that are suitable for ICP-OES detection.[5] Most of these suitable emission lines are observed in the ultraviolet-visible range of the electromagnetic spectrum. The number of prominent emission lines varies for each element as does the detection limit for each emission line. Line selection is based on intensity of the emission lines, as well as the number of interfering lines from other elements present in the sample.

ICP-OES instruments show elevated background levels for some elements and have relatively higher detection limits compared to other techniques, such as graphite furnace atomic emission spectroscopy. ICP-OES does have advantages in its wide spectral range, high throughput, precision, and operating costs that are low compared to inductively coupled plasma-mass spectrometry (ICP-MS).

2.3 Inductively Coupled Plasma-Mass Spectrometry

Inductively coupled plasma-mass spectrometry (ICP-MS) is an elemental analysis technique used for the same types of samples as ICP-OES, but benefits from detection limits up to three orders of magnitude lower than ICP-OES.[9]

The sample introduction process and plasma formation for ICP-MS is similar to that described for ICP-OES. In an ICP-MS instrument, desolvation and atomization still occur in the plasma torch; however, it is the formation of ions as opposed to thermal excitation that is required for mass analysis. In the plasma torch, ionization of the ground state atoms occurs via collisions with the argon ions and electrons that form the plasma.[8]

As shown in Figure 2.3, a mass spectrometer consists of a low vacuum region and a high vacuum region separated in this case by an octopole. Since the ionization takes place at atmospheric pressure and the mass analyzer is maintained at low pressure (10^{-5} Torr), a differential pumping system is required between the ionization chamber and the mass analyzer.

The sample ions, which are singly charged, positive ions, are directed from the torch through the atmospheric pressure interface and the octopole in to the mass analyzer, where ions are separated by their mass-to-charge ratio (m/z). Ions produced in the plasma torch are directed between low and high vacuum regions through skimmer cones. Skimmer cones are lenses with orifices small enough to maintain proper vacuum pumping, but large enough to allow the passage of ions to reach optimal sensitivity. The octopole operates in an RF-only mode, which will be described later, in order to serve as an ion guide to efficiently transport ions from the low to high vacuum regions of the spectrometer.

A common mass analyzer in an ICP instrument is a linear quadrupole that separates ions by scanning the amplitudes of constant and oscillating applied potentials. Only ions with m/z values that are stable under these applied potentials will traverse the length of the quadrupole and reach the detector. The quadrupole is composed of two pairs of cylindrical (ideally hyperbolic) rods that lie parallel to one another. One pair of parallel rods is connected to the positive side of a direct current (DC) source and the second pair of rods is connected to the negative terminal.[5] Two alternating current (AC) radio frequency (RF) voltages that are 180° out of phase with one another are also applied to each pair of rods. Upon reaching the mass analyzer, the ions are accelerated into an electric field formed in the center of the four electrode rods that make up the quadrupole.[9] The pairs of rods operate as mass filters to allow passage of ions in a narrow m/z

range. In the absence of a DC potential, the rods in the x-z plane (Fig. 2.4) alternately attract and repel the positively charged ions during the negative and positive cycles of the RF potential, respectively. Since the trajectories of ions depend on the mass and momentum of the ions and momentum is directly proportional to the square root of the ion mass, a heavier ion will maintain a stable trajectory through the quadrupole.[5] Alternatively, a lower mass ion's trajectory will be influenced by the RF potential and will travel a distance that exceeds the quadrupole field radius (r_0) causing intersection with the rods and formation of a neutral species. Therefore, the positively charged rods in the x-z plane form a high pass mass filter. Operating in the RF-only mode allows ions in a specified mass range to be guided through a multipole, such as the quadrupole or octopole, without collision into the rods.[9] In the absence of an AC potential, the negatively biased rods in the y-z plane will attract the ions moving through the quadrupole. The addition of the RF field will counteract the attraction towards the negative rods for low mass ions, but cannot redirect high mass ions, making the negative rods a low pass mass filter.[10]

A quadrupole mass analyzer is capable of resolving ions with m/z values differing by one unit by scanning the amplitudes of the AC and DC voltages from zero to a maximum value. The best resolution is achieved when a constant AC to DC voltage ratio is maintained.[10] Positive ions maintaining a stable trajectory through the quadrupole pass through an exit slit and are collected and converted into an electrical signal by a transducer, typically an electron multiplier.[5] An electron multiplier is made up of a series of discrete dynodes with successively higher applied potentials or a continuous dynode with a potential gradient. The collision of a positive ion with a dynode will cause multiple electrons to be emitted.

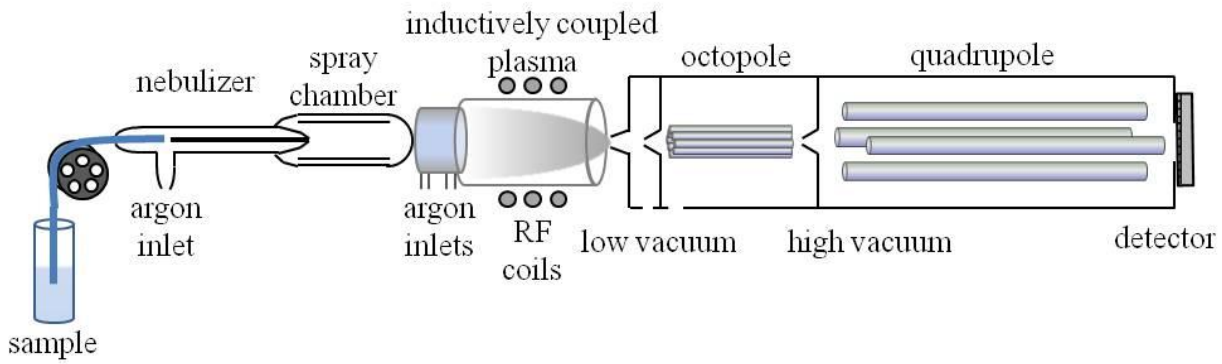

Figure 2.3 Schematic of inductively coupled plasma-mass spectrometer.

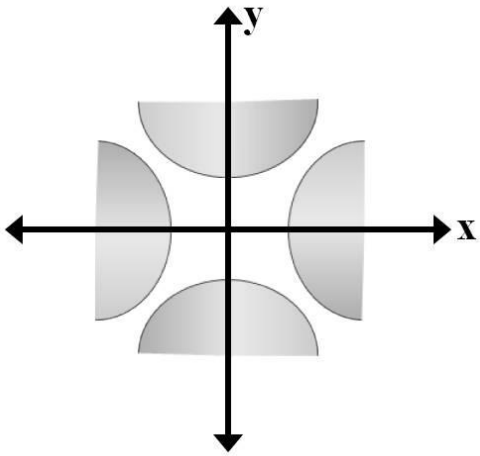

Figure 2.4 Cross-sectional view of quadrupole mass analyzer showing x and y dimensions.

The secondary electrons will then be attracted toward higher voltage dynodes resulting in the ejection of more electrons leading to a cascade of electrons and amplification of the signal. The measured current is recorded as a count rate for each element and the count rate is proportional to the element's concentration allowing for quantification. Ion counting by electron multipliers results in a limited dynamic range typically five orders of magnitude. The limited dynamic range is caused by the inability of the measurement circuitry to detect both high and low ion counts.[11] In order to extend the dynamic range, the detector is set up to simultaneously detect low counts by the traditional operation of the dynodes and detect high counts via analog detection. An analog signal is triggered when the ion signal reaches a specified threshold and occurs when the cascade of electrodes reaches a midpoint in the dynode.[11] Simultaneous ion counting and analog detection extends the ICP-MS dynamic range up to nine orders of magnitude.

ICP-MS instruments have relatively low background signals compared to ICP-OES, which can have elevated and structured requiring background correction. Low background is a major reason for the lower detection limits of ICP-MS. ICP-MS does have limitation in that it has a higher incidence of matrix interferences and requires addition of multiple internal standards. Another notable difference in the two techniques is capital and operating costs. ICP-MS has a higher up-front cost and higher operating costs due to replacing components with limited lifetimes. Table 2.1 shows a comparison of ICP-OES and ICP-MS instrument capabilities and costs. Detection limit ranges are lower for ICP-MS, which also has a wider analytical range; however ICP-OES has a higher limit for the analytical working range and is able to detect higher element concentrations without sample dilution. Both techniques are capable of multi-element analysis and able to determine 73 elements per minute in a single sample.

Table 2.1 Typical instrument capabilities and purchase costs for inductively coupled plasma-optical emission spectroscopy (ICP-OES) and inductively coupled plasma-mass spectrometry (ICP-MS)

Specification	ICP-OES†	ICP-MS†
Detection Limit Range (µg/L)	0.05 – 10	<0.001 – 1
Analytical Working Range (Orders of magnitude)	6	9
Sample Throughput (Elements/min)	73	73
Cost (Purchase price, $US)	$60 – 100K	$130 – 200K

†Available from: http://www.perkinelmer.com/PDFs/Downloads/BRO_WorldLeaderAAICPMSICPMS.pdf .

2.4 Statistical Methods

Student's t-tests are utilized to assess statistical differences in two mean values, for example, two mean elemental concentrations determined for different bullet types. Assuming a normal distribution, the two-tailed, pooled t-test is used for samples sets with equal variance.[12] The variance (s^2) is equal to the square of the standard deviation of a mean and is a measure of the spread in replicate measurements as shown in Equation 4.1,

$$s^2 = \frac{\sum_{i=1}^{n} (x_i - \bar{x})^2}{(n-1)} \tag{4.1}$$

where x_i is the value of one sample, $\bar{x}$ is the mean of the population and n is the number of samples in the population. The t-statistic is calculated from the difference in the two sample means, $\bar{x}_1$ and $\bar{x}_2$, and the pooled standard error (Eqn. 4.2).

$$t = \frac{|\bar{x}_1 - \bar{x}_2|}{s_{pooled}} \sqrt{\frac{n_1 n_2}{n_1 - n_2}} \tag{4.2}$$

The pooled standard error takes into account the pooled standard deviation, s_{pooled}, and the sample populations n_1 and n_2. The degrees of freedom for the pooled t-test is $n_1 + n_2 - 2$.

$$s_{pooled} = \sqrt{\frac{{s_1}^2 (n_1 - 1) + {s_2}^2 (n_2 - 1)}{n_1 + n_2 - 2}} \tag{4.3}$$

The pooled standard deviation is shown in Equation 4.3, where s_1 and s_2 are the standard deviations of sample sets 1 and 2, respectively. The calculated t-statistic is compared to the critical t-value at a desired confidence level. A t-statistic that is greater than the critical t-value indicates a significant difference in the sample means at the specified confidence level.

A method to evaluate the strength of linear association between two variables, such as the association of concentrations of lead and antimony for a given combination of bullet and firing distance, is to calculate the Pearson product moment correlation (PPMC) coefficients.[13] PPMC coefficients are calculated as shown in Equation 4.4,

$$r = \frac{\sum_{i=1}^{n}(x_i - \bar{x})(y_i - \bar{y})}{\sqrt{\sum_{i=1}^{n}(x_i - \bar{x})^2 \sum_{i=1}^{n}(y_i - \bar{y})^2}} \tag{4.4}$$

where r is the PPMC coefficient, $\bar{x}$ is the mean of one population and $\bar{y}$ is the mean of a second population. PPMC coefficients range in value from -1 to +1, where negative values indicate a negative correlation and positive values indicate a positive correlation. The sign and strength of the PPMC coefficient allows inference about the relationship between populations and allows for a predictive model to be applied. For example, a strong positive correlation means a both increase together and a linear relationship can be used to model the two populations. The gradations of correlation strength are as follows: a PPMC coefficient of ±0.8–1 is considered a strong correlation, ±0.5–0.79 is a moderate correlation, ±< 0.49 is a weak correlation, and zero indicates no correlation between the two variables of interest.[14]

REFERENCES

REFERENCES

1. Lamble KJ, Hill SJ. Microwave digestion procedures for environmental matrices. Analyst. 1998; 123:103R-33R.

2. Arruda MAZ, editor. Trends in sample preparation. New York: Nova Science Publishers, 2007.

3. Abu-Samra A, Morris JS, Koirtyohann SR. Wet ashing of some biological samples in a microwave oven. Anal Chem. 1975; 47:1475-7.

4. Sandroni V, Smith CMM. Microwave digestion of sludge, soil and sediment samples for metal analysis by inductively coupled plasma-atomic emission spectrometry. Anal Chim Acta. 2002; 468:335-44.

5. Skoog DA, Holler FJ, Crouch SR. Principles of instrumental analysis. 6th ed. Belmont, CA: Thomson Brooks/Cole, 2007.

6. Sharp BL, Chenery S, Jowitt R, Fisher A, Sparkes ST. Atomic spectrometry update - atomic-emission spectrometry. J Anal At Spectrom. [Review]. 1995; 10:R139-R71.

7. Thomas R. Spectroscopy tutorial - a beginner's guide to icp-ms - part iii: The plasma torch. Spectroscopy. 2001; 16:26-30.

8. Montaser A, Golightly DW, editors. Inductively coupled plasmas in analytical atomic spectrometry. 2nd ed. New York: Wiley-VCH, 1992.

9. de Hoffmann E, Stroobant V. Mass spectrometry: Principles and applications. 3rd ed. Chichester, West Sussex, UK: John Wiley & Sons, Ltd, 2007.

10. Miller PE, Denton MB. The quadrupole mass filter - basic operating concepts. J Chem Educ. 1986; 63:617-22.

11. Thomas R. Spectroscopy tutorial - a beginner's guide to icp-ms - part x: Detectors. Spectroscopy. 2002; 17:34-9.

12. Harris DC. Exploring chemical analysis. 2nd ed. New York: W.H. Freeman, 2001.

13. De Veaux R, Velleman P, Bock D. Intro stats. 2nd ed. Boston: Pearson Addison Weasley, 2006.

14. Peck R, Olsen C, Devore J. Introduction to statistics and data analysis. 3rd ed. Belmont, CA: Brooks/Cole, 2009.

Chapter 3: Materials and Methods

3.1 Experimental Design

The current study was designed to compare elemental composition and concentration in gunshot residue (GSR) deposited on fresh porcine tissue and collected throughout the stages of decomposition. The bullet types and the firing distances used in the GSR deposition were varied. This study also investigated the utility of inductively coupled plasma-optical emission spectroscopy (ICP-OES) to detect the elemental composition of GSR over time compared to inductively coupled plasma-mass spectrometry (ICP-MS).

In September 2011, four euthanized pigs were obtained from the Michigan State University (MSU) Swine Teaching & Research Center and treated in accordance with the Institute for Animal Care and Use Committee (IACUC) guidelines. The pigs ranged in size from 90 to 120 pounds. A .357 magnum Dan Wesson® revolver (blued steel barrel, 1.5 inch in length) was used to deposit GSR on the pigs. The first pig was shot six times with non-jacketed (NJ) bullets at a firing distance of 5 cm (Fig. 3.1).

The second pig was shot at a firing distance of 10 cm with NJ bullets. The third and fourth pigs were shot six times with full-jacketed (FJ) bullets at firing distances of 5 and 10 cm, respectively. The shot entrance wounds were spaced approximately 20 cm apart. The propellant was hand loaded and, therefore, was consistent between the NJ and FJ ammunition. The barrel of the firearm was cleaned between shots of the same bullet type, whereas the barrel and the chamber of the firearm were cleaned between firings of the different bullet types.

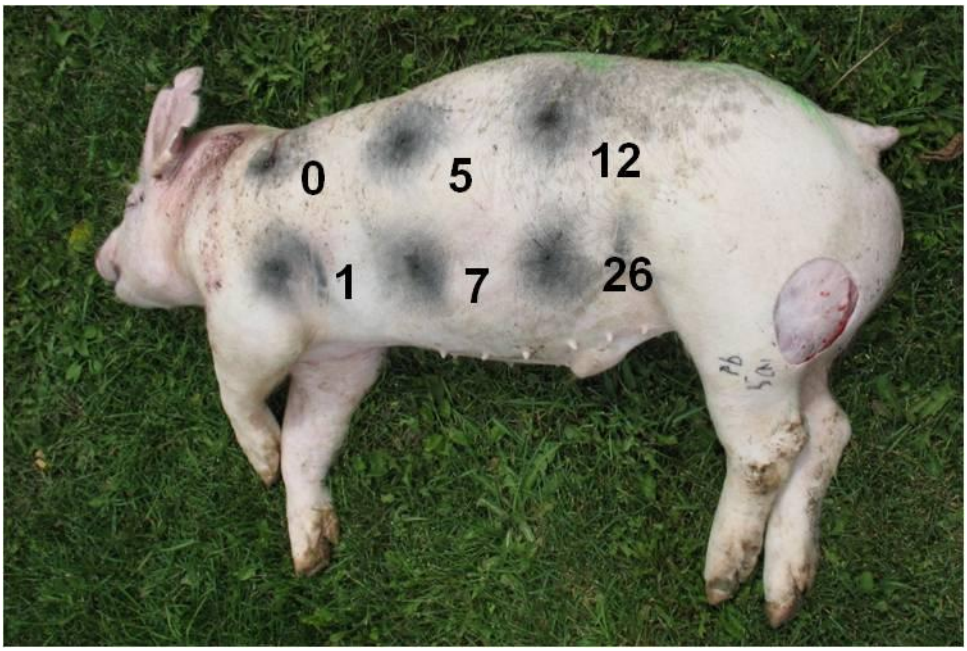

Figure 3.1 Gunshot wounds with gunshot residue deposited by non-jacketed ammunition at a 5 cm firing distance. The wounds are labeled with the number of days since death that each wound was collected.

Fresh control samples were collected from each pig prior to GSR deposition. The tissue and underlying fat surrounding one gunshot wound was collected from each pig immediately after GSR deposition as a fresh sample. All wounds were excised with sterile, stainless steel scalpels (BD Bard-Parker, Franklin Lakes, NJ). The excised tissue samples containing GSR varied in size depending on the size of the GSR pattern, but were in the range from 5 to 10 cm in diameter. Excised wounds were loosely wrapped in waxed paper, placed in a plastic zip top bag, and were stored at -80 °C until analysis. All fresh samples were labeled as Day 0 and also labeled with the collection date, bullet type, and firing distance. The pigs were housed in wire cages designed to allow for natural decomposition and to protect from predatory mammals for the duration of the study.

On the first day of decomposition, Day 1, a second wound was collected from each pig. The two gunshot wounds closest to the head of the pig were collected first since the insect activity is often initiated in the orifices of the head. The four remaining wounds were collected on Days 5, 7, 12, and 26. Control tissue was collected from either the hind leg or hind quarters of the pig on Days 5, 12, and 26. The average temperature during the study was 57 °F with a high of 83 °F and a low of 36 °F. The total precipitation over the 26 day period was 2.09 inches. A full summary of the environmental conditions recorded during the study is presented in Appendix A.

3.2 Microwave-Assisted Digestion of Porcine Tissue

The excised gunshot wounds were brought to room temperature prior to sampling and weighing. A scalpel was used to cut a tissue section from directly adjacent to the entry wound. The tissue samples had masses between 0.30 and 0.55 g. The control tissue samples were prepared in the same manner. Each tissue sample was placed into an individual 30 mL quartz

vessel with 2 mL of 70% nitric acid (Optima grade, Fisher Scientific, Pittsburgh, PA) and 1 mL 30% hydrogen peroxide (J.T. Baker, Mallinckrodt, Inc., Phillipsburg, PA). Each quartz vessel was capped and placed inside a 100 mL teflon vessel with 2 mL 30% hydrogen peroxide and 10 mL distilled water. A thermowell came into contact with the liquid in the teflon vessel to monitor the temperature with a thermocouple in the reference vessel. One quartz vessel from each digestion run was used as a procedural blank and contained only nitric acid and hydrogen peroxide. The teflon vessels were placed in the microwave sample holder and the lids were tightened. An Ethos EX closed vessel microwave solvent extraction labstation with SK-10 high pressure rotor (Milestone Inc., Shelton, CT) was used to digest all samples. The microwave temperature was initially ramped from room temperature to 210 °C at 15 °C/min and then held at 210 °C for 10 min. The power was held at 1000 W. The temperature program and power were previously utilized for paper[1] and tissue[2] digestion. All sample vessels were allowed to cool prior to transfer of the digests. The concentrated digests were stored in polypropylene conical vials (Corning Inc., Corning, NY) at 4 °C until further dilution and analysis. Quartz vessels were cleaned with nitric acid and hydrogen peroxide between microwave digestion runs.

3.3 ICP-OES Elemental Analysis

The concentrated digests were initially diluted to a 2% nitric acid solution for ICP-OES analysis by adding 0.5 mL digest to 11.167 mL pure water in order to decrease the acid concentration for the analysis. The samples were further diluted by a factor of 25 by adding 0.4 mL of the dilute digest solution to 10 mL 2% nitric acid. The second dilution was required to adjust the element concentrations to within the instrumental working range. Mixed element standards were prepared with concentration ranges of micrograms per liter (μg/L) for calibration. The concentration range for lead (Pb) and antimony (Sb) was 2.5–10,000 μg/L, while the

concentration range for barium (Ba), copper (Cu), iron (Fe), and zinc (Zn) was 5–500 ug/L. All standards were prepared in glassware washed in 2% nitric acid.

An ICP-OES Varian 710-ES Axial spectrometer (Agilent Technologies, Santa Clara, CA) with ICP Expert^{TM} II software was used for the analysis. Operating parameters are shown in Table 3.1. The emission lines selected were 220.353 nm for Pb, 206.834 nm and 231.146 nm for Sb, 455.403 nm for Ba, 327.395 nm for Cu, 238.204 nm for Fe, and 206.200 nm and 213.857 nm for Zn. For elements with low first ionization potentials such as Ba, the emission occurs after ionization. The ionic and atomic emission lines are shown in Table 3.2. These lines were chosen based on the intensity of emission, as well as the possible presence of elements with interfering emission lines. Two lines were selected for Sb and Zn as the line of maximum intensity had possible interferences from other elements. The emission intensity of the digest samples and element standards were measured in triplicate. Blank samples were measured periodically throughout the analysis to assess instrument carryover. One set of standards was analyzed before the tissue samples and one set analyzed at the end of the analysis to assess instrumental drift. Instrumental drift was calculated as the percent difference between two sets of standards analyzed approximately one hour apart.

Table 3.1 ICP-OES Varian 710-ES instrument parameters/operating conditions

ICP-OES operating parameters	
RF Power (W)	1000
Plasma gas flow (L/min)	15
Auxiliary gas flow (L/min)	1
Nebulizer pump (rps)	0.25
Replicate read time (s)	5
Uptake delay (s)	30
Echelle grating (lines/mm)	94.74

Table 3.2 Element emission lines for ICP-OES analysis

Element (Symbol)	Emission line(s) (nm)
Lead (Pb)	220.353[i]
Antimony (Sb)	206.834[i], 231.146[a]
Barium (Ba)	455.403[i]
Copper (Cu)	327.395[a]
Iron (Fe)	238.204[i]
Zinc (Zn)	206.200[i], 213.857[a]

i = ionic emission line, a = atomic emission line

3.4 ICP-MS Elemental Analysis

The concentrated digests were initially diluted for ICP-MS analysis by adding 0.5 mL digest to 0.67 mL pure water. The samples were further diluted by a factor of 20 by adding 0.05 mL of the dilute digest solution to 1 mL 20% nitric acid. The first dilution was done to decrease the acid concentration, while the second dilution was required to adjust the element concentrations to within the instrumental working range. Mixed element standards were prepared for calibration. The concentration range for Pb and Sb was 0.1–10,000 µg/L, while the concentration range for Ba, Cu, Fe, and Zn was 0.05–500 ug/L. All standards were prepared in acid washed glassware with 2% nitric acid. For ICP-MS analysis 200 µL of sample was pipetted into a plastic test tube and 6 mL of an internal standard diluent was added to each sample. The internal standard diluent contained 10 µg/L scandium (^{45}Sc), 15 ug/L germanium (^{74}Ge), rhodium (^{103}Rh), indium (^{115}In), and bismuth (^{209}Bi), as well as 2% butanol, 0.05% Triton X-100 and EDTA, and 1% ammonium hydroxide. The high acid concentration in the ICP-MS samples was diluted when the internal standard diluent was added.

The ICP-MS was an Agilent 7500 Series (Agilent Technologies, Santa Clara, CA) equipped with a CETAC autosampler and ChemStation software. The detection was accomplished by a simultaneous pulse counting and analog detector, which allowed for a linear dynamic range of up to nine orders of magnitude. Instrument operating parameters are presented in Table 3.3. Standard reference samples were used to tune the ICP-MS and assess accuracy, precision, and resolution. The nominal and isotopic masses for each element studied are shown in Table 3.4.

Table 3.3 ICP-MS Agilent 7500 instrument parameters/operating conditions

ICP-MS operating parameters			
Torch-H (mm)	0.6	**Quadrupole parameters**	
Torch-V (mm)	0.3	**AMU gain**	134
Argon flow rates		**AMU offset**	128
Carrier gas (L/min)	0.82	**Axis gain**	1.0005
Makeup gas (L/min)	0.2	**Axis offset**	-0.05
Nebulizer pump (rps)	0.22	**QP bias (V)**	-3
S/C temperature (°C)	2	**Detector parameters**	
Ion lenses		**Discriminator (V)**	8
Extract 1 (V)	0	**Analog HV (V)**	1780
Extract 2 (V)	-125	**Pulse HV (V)**	1580
Omega bias-ce (V)	-24	**Acquisition parameters**	
Cell entrance (V)	-26	**Mode (nongas)**	
QP Focus (V)	2	**Integration time (s) (per point, per mass)**	
Cell exit (V)	-30	**^{137}Ba**	0.10, 0.30
Octopole parameters		**^{56}Fe, ^{65}Cu, ^{66}Zn**	0.30, 0.90
Octopole RF (V)	150	**^{121}Sb, ^{208}Pb**	0.50, 1.5
Octopole bias (V)	-6		

Table 3.4 Element nominal and isotopic masses for ICP-MS analysis

Element (Symbol)	Nominal mass	Isotopic mass (amu)
Lead (Pb)	208	207.977
Antimony (Sb)	121	120.904
Barium (Ba)	137	136.906
Copper (Cu)	65	64.928
Iron (Fe)	56	55.935
Zinc (Zn)	66	65.926

3.5 Data Analysis Methods

The ICP-OES analysis of the elemental standards and tissue samples resulted in triplicate measurements of spectral intensity for all elements in each sample. A standard calibration curve was prepared for each element using average intensities of the blanks and standards prepared as described in section 3.3. The standard curves for Ba, Cu, Fe, and Zn were constructed from a blank and six standards ranging in concentration from 5–500 μg/L, while the standard curves for Pb and Sb were constructed from a blank and eight standards ranging in concentration from 10–10,000 μg/L. The different concentration ranges selected were based on a preliminary analysis of the elemental composition of the tissue samples. The quality of the calibration was assessed by calculating the percent relative standard deviation (RSD) for each calibration standard. The limit of detection (LOD) for each element was calculated as 3 standard deviations of the calibration blank. Another analytical figure of merit, sensitivity, was determined from the slope of the calibration curve.

The element concentrations for each replicate of the control tissue and GSR tissue samples were calculated using the slope and the y-intercept of the respective element's standard curve. The calculated triplicate element concentrations were multiplied by dilution factors, averaged, and standard deviations were calculated. All tissue sample elemental concentrations determined in μg/L were normalized to the mass of tissue analyzed resulting in concentrations in μg element per gram of tissue. The procedural blank concentrations were determined in a similar manner, but were not normalized to mass, as no tissue was present in these samples. Student's t-tests were employed for ICP-OES data to assess differences in elemental concentration between two samples and to differentiate bullet types and firing distances based on element concentration.

A two-tailed, pooled t-test was used to calculate the t-statistic which were compared with critical t-values at confidence levels between 80–99.9%.[3]

The ICP-MS analysis of the elemental standards and tissue samples resulted in counts per second (cps) values for each element in each sample. The cps for ^{56}Fe, ^{65}Cu, and ^{66}Zn were normalized to the ^{115}In internal standard peak, while ^{121}Sb, ^{137}Ba, and ^{208}Pb were normalized to the ^{209}Bi internal standard peak. Standard curves were prepared with the normalized values from the standards prepared as described in section 3.3. The standard curves for Ba, Cu, Fe, and Zn were constructed from a blank and seven standards ranging in concentration from 2.5–500 μg/L, while the standard curves for Pb and Sb were constructed from a blank and nine standards ranging in concentration from 5–10,000 μg/L. The elemental concentrations for the procedural blanks, control tissue, and GSR tissue were calculated from the slopes and intercepts of the standard curves. As was the case with the ICP-OES data, the tissue concentrations were multiplied by dilution factors and normalized to the mass of tissue. Analytical figures of merit of sensitivity and limit of quantitation (LOQ) were assessed. The LOQ was determined to be the concentration of the lowest linear point on the calibration curve. No replicates were obtained during the ICP-MS analysis and limited statistical procedures were possible. The strengths of linear associations between ICP-MS elemental concentrations were evaluated by calculating Pearson product moment correlation (PPMC) coefficients between pairs of elements.

APPENDIX

Table 3.5 Weather conditions including temperature and precipitation recorded during the duration of the study with sample collection days indicated with an x

Day	Date	Temperature (°F) Max.	Min.	Average	Precipitation (in)	Samples Collected	Controls Collected
0	9/7/2011	67	48	58	trace	x	x
1	9/8/2011	65	55	60	trace	x	
2	9/9/2011	76	59	68	0.24		
3	9/10/2011	79	61	70	0.01		
4	9/11/2011	78	59	69	-		
5	9/12/2011	83	61	72	-	x	x
6	9/13/2011	76	50	63	-		
7	9/14/2011	67	41	54	0.23	x	
8	9/15/2011	59	36	48	-		
9	9/16/2011	58	37	48	-		
10	9/17/2011	66	46	56	-		
11	9/18/2011	70	42	56	trace		
12	9/19/2011	68	51	60	0.47	x	x
13	9/20/2011	70	47	59	-		
14	9/21/2011	76	54	65	-		
15	9/22/2011	68	52	60	-		
16	9/23/2011	64	48	56	-		
17	9/24/2011	66	44	55	trace		
18	9/25/2011	70	49	60	0.04		
19	9/26/2011	69	47	58	0.30		
20	9/27/2011	65	45	55	0.18		
21	9/28/2011	62	52	57	0.04		
22	9/29/2011	63	49	56	0.39		
23	9/30/2011	52	40	46	0.19		
24	10/1/2011	54	36	45	-		
25	10/2/2011	62	34	48	-		
26	10/3/2011	68	38	53	-	x	x

http://www.crh.noaa.gov/product.php?site=grr&product=cli&issuedby=lan.
Daily climate (Lansing)

REFERENCES

REFERENCES

1. McGaw EA, Szymanski DW, Smith RW. Determination of trace elemental concentrations in document papers for forensic comparison using inductively coupled plasma-mass spectrometry. J Forensic Sci. 2009; 54:1163-70.

2. LaGoo L, Schaeffer LS, Szymanski DW, Smith RW. Detection of gunshot residue in blowfly larvae and decomposing porcine tissue using inductively coupled plasma mass spectrometry (icp-ms). J Forensic Sci. 2010; 55:624-32.

3. De Veaux R, Velleman P, Bock D. Intro stats. 2nd ed. Boston: Pearson Addison Weasley, 2006.

Chapter 4: Results and Discussion

4.1 Decomposition Observations

Over a period of 27 days in the fall of 2011, the decomposition of four pigs shot with different bullet type and firing distance was monitored while samples of tissue were collected. The amount of visible gunshot residue (GSR) deposited on the porcine tissue was observed to vary between the different firing distances (5 cm and 10 cm) and between the different bullet types (non-jacketed (NJ) and full-jacketed (FJ)) (Fig. 4.1). The GSR pattern distributed around the entry wounds on the pigs shot with NJ bullets was larger in diameter than that observed on pigs shot with FJ ammunition and the amount of soot closest to the entry wounds was also observed to be greater for wounds made with NJ bullets. Shots fired with NJ ammunition at 5 cm (Fig. 4.1A) had GSR patterns that were increased in diameter compared to shots fired from 10 cm (Fig. 4.1B), but the amount of residue closest to the entry wound was visibly similar for both firing distances. For the FJ GSR deposition, there was a slightly larger GSR pattern deposited from a 5 cm firing distance (Fig. 4.1C) compared to 10 cm (Fig. 4.1D), while there was an increased amount of soot visible on the FJ 5 cm wound.

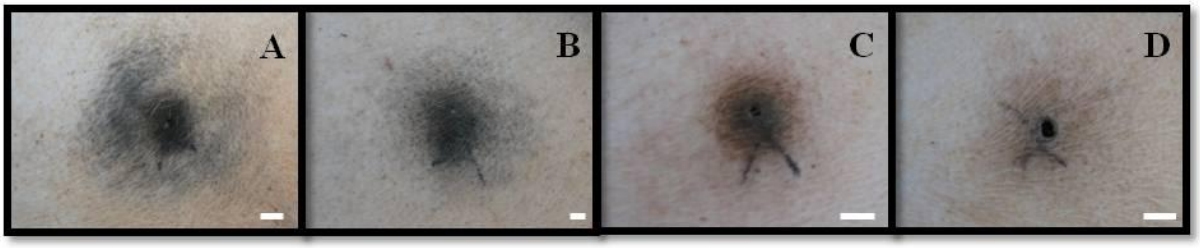

Figure 4.1 Gunshot residue deposited with (A) non-jacketed (NJ) ammunition at 5 cm, (B) NJ ammunition at 10 cm, (C) full-jacketed (FJ) ammunition at 5 cm, and (D) FJ ammunition at 10 cm. Scale bar width represents 1 cm.

The four pigs used in this study were all exposed to the same environmental conditions; however, variable rates of decay were observed. Decomposition is considered a continuum process starting with death and ending with skeletonization, but there are documented stages defined within this continuum.[1] These stages of decomposition, which include fresh, bloat, active decay, advanced decay and desiccation will be used as reference points for the discussion of decomposition. Following death, biochemical processes including respiration and cellular oxidative phosphorylation cease and molecules supplying energy to cells, such as adenosine triphosphate (ATP), are no longer produced.[2] The consequence of this is the initiation of autolytic processes, which include the enzymatic breakdown of cells. Early decomposition phenomena, rigor mortis and livor mortis, occur within a few hours after death. Rigor mortis is observed as the stiffening of muscles and is the result of a decrease in molecules providing energy to the cells. Muscle proteins, actin and myosin, are part of a complex that requires ATP to dissociate for normal muscle contraction.[3] In addition, calcium ions bind to a protein, troponin, which causes a conformational change in myosin that allows actin and myosin to bind and form a complex. The ATP depleted environment and the breakdown of organelles that store calcium ions causes the association and dissociation cycle of the actin-myosin complex in muscles to cease resulting in the muscle stiffness observed after death.[2] Livor mortis is characterized by the coloration that occurs as deoxygenated blood settles to the lowest portion of the carcass.[1] For all four pigs, the initial stages of decomposition including rigor mortis and livor mortis were observed on Day 0 within a few hours of euthanization. The remaining stages are described below, case by case for each pig.

The decomposition of the pig shot with NJ ammunition at a 5 cm firing distance is described first. This pig, denoted NJ 5 cm, was the smallest of the four pigs weighing approximately 90 pounds. Selected images taken throughout decomposition are shown in Figure 4.2. As stated previously, rigor mortis and livor mortis were observed within the first few hours after euthanization. The carcass reached the bloat stage by Day 3 and blowfly larvae were active in the mouth on Day 5. The bloat is a sign of putrefaction, which is characterized by growth of primarily anaerobic bacteria in the abdomen.[2] Production of gases and other metabolites by bacteria causes the build-up of gases in the carcass, which results in the characteristic bloating. A combination of initial bloating and rigidity followed by a decrease in rigidity caused the center mass of the carcass to rotate so the underbelly was exposed and the shot tissue was positioned closer to the ground as shown in Figure 4.2B and C. A consequence of the carcass position was the shots collected on Days 5 and 12 (see Fig. 3.1) were in close proximity to the larval mass present on the ground next to the carcass, which may have affected the GSR to a different extent compared to the shots collected on Days 7 and 26. Blowfly larvae were present in the orifices of the head on Day 7, in the control wounds on Day 10, and covered three quarters of the mass of the carcass by Day 19. A significant mass loss occurred between Day 19 and Day 26 due in large part to larval feeding. The skeleton was almost fully exposed by Day 26 when the last tissue sample was collected. The tissue collected on Day 26 was black in color, but not completely dried. The location of the tissue collected on Day 26 is marked with a white arrow in Figure 4.2D.

The pig shot with NJ ammunition at a firing distance of 10 cm was denoted NJ 10 cm and was approximately 110 pounds (Fig. 4.3). The carcass reached the bloat stage on Day 1 and blowfly larvae were observed in the excised wounds and on the head by Day 5. The rotation of

the carcass after bloating described for the NJ 5 cm pig was also observed for the NJ 10 cm pig as shown in Figure 4.3C. Active decay followed by advanced decay continued through Day 18 with skin slippage observed on Day 8. Active decay is characterized by feeding of insect larvae and loss of mass, whereas advanced decay is characterized by reduced larvae activity and death of surrounding vegetation due to liquids released during active decay.[4] Desiccation of the skin, which is evident in Figure 4.3D, was observed as early as Day 10 at which time the skin on the carcass appeared leathery and dark in color.

Figure 4.2 Gunshot residue deposited with non-jacketed ammunition at a firing distance of 5 cm on porcine tissue shown (A) 0, (B) 7, (C) 12, and (D) 26 days after death. The tissue sample collected on Day 26 is indicated by an arrow in (D).

Figure 4.3 Gunshot residue deposited with non-jacketed ammunition at a firing distance of 10 cm on porcine tissue shown (A) 0, (B) 7, (C) 12, and (D) 26 days after death.

The pig shot with FJ ammunition at a firing distance of 5 cm, denoted FJ 5 cm, was approximately 110 pounds and had a similar progression in decomposition to the NJ 10 cm pig (Fig. 4.4). On Day 3, the carcass was bloated and blowfly larvae were observed in the mouth on Day 4. Carcass rotation caused the wounds to be positioned closer to the ground as shown in Figure 4.4B and C. Skin slippage was observed on the back of the carcass on Day 6. Active decay progressed with blowfly larvae activity moving from the head into the excised wounds and then leaving the carcass by Day 18. As was observed with the NJ 10 cm pig, desiccation started on Day 10.

The largest pig weighed approximately 120 pounds and was shot with FJ ammunition at a firing distance of 10 cm (Fig. 4.5). This pig was denoted FJ 10 cm and decomposed to a lesser extent compared to the other three pigs. Livor mortis was observed within a few hours of euthanization. The carcass reached a bloat stage on Day 3. Blue discoloration and marbling were observed on Day 4. The mouth and portions of the head of the carcass were partially obscured by tall grass, so the first blowfly larvae observed in the wounds was on Day 11. Active decay continued with the larvae encompassing a larger area of the carcass by the last day of the study, Day 26.

In addition to the natural decomposition processes and insect activity described above, environmental conditions, as well as shot locations affected the persistence of GSR. All four pigs were exposed to the same environmental conditions, which included approximately 2 inches of precipitation; however, some gunshot wounds were less exposed. The rotation of some of the carcasses, described previously, shielded some of the gunshot wounds from direct precipitation, but allowed for the possibility of water to wash over the remaining GSR. Shot location was also

pertinent to the persistence of GSR when body fluids, including blood or stomach contents, were released via the gunshot wounds as shown in Fig. 4.5C.

Figure 4.4 Gunshot residue deposited with full-jacketed ammunition at a firing distance of 5 cm on porcine tissue shown (A) 0, (B) 7, (C) 12, and (D) 26 days after death.

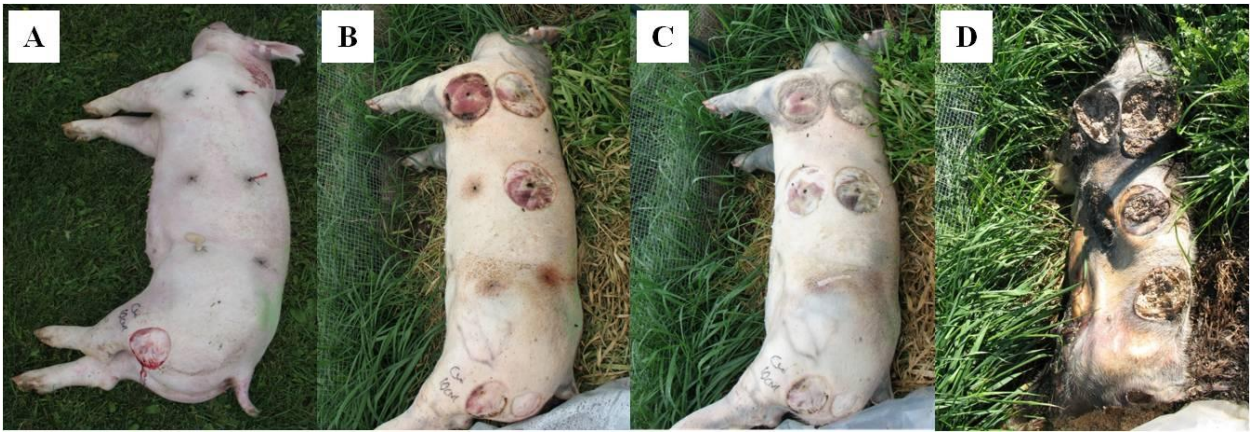

Figure 4.5 Gunshot residue deposited with full-jacketed ammunition at a firing distance of 10 cm on porcine tissue shown (A) 0, (B) 7, (C) 12, and (D) 26 days after death.

4.2 Fresh Tissue Studies

The fresh tissue samples collected immediately after GSR deposition on Day 0 were prepared as described in section 3.2 and analyzed by inductively coupled plasma-optical emission spectroscopy (ICP-OES), as well as inductively coupled plasma-mass spectrometry (ICP-MS).

4.2.1 ICP-OES Analysis of Fresh Tissue Samples

First, the calibration of element standards for each spectral emission line, quantitation of elements and analytical figures of merit were assessed for the ICP-OES analysis. Multiple spectral emission lines were available for each of the six elements analyzed, lead (Pb), antimony (Sb), barium (Ba), copper (Cu), iron (Fe), and zinc (Zn). A single emission line was selected for analysis of Pb, Ba, Cu, and Fe. All of these lines were the highest intensity line available for analysis for each element and had few interfering lines associated with common sources of contamination. The selected lines for Sb and Zn were close in wavelength, so additional lines at 231.146 nm for Sb and 213.857 nm for Zn were analyzed. The calibration curve for each line was assessed and the results from the most intense lines, 206.833 nm and 206.200 nm for Sb and Zn, respectively, were selected for further analysis. The emission lines selected for each element along with the potential interfering elements are listed in Table 4.1. No evidence of interference from Sb was observed in the calibration curve for Zn or vice versa. A majority of the interfering elements listed in Table 4.1 have not been shown to have a coincidence with the elements found in GSR with the exception of cobalt (Co) and zirconium (Zr). Cobalt and Zr have been used in some ammunition primers, but are rarely found in primers formulated with Pb, Sb, and Ba compounds.[5] Although some of the other interfering elements are found in the environment, contamination from elements found in environmental sources including chromium (Cr) found in

dyes and pigments and bismuth (Bi) used in some pharmaceuticals was unlikely under the conditions of the experiment.

Table 4.1 ICP-OES spectral emission lines and potential elemental interferences

Element	Emission Wavelength (nm)	Interfering Elements†
Lead (Pb)	220.353	Bi, Nb
Antimony (Sb)	206.834	Ta, Cr, Ge, Hf
Barium (Ba)	455.403	Zr, U
Copper (Cu)	327.395	Nb, U, Th, Mo, Hf
Iron (Fe)	238.204	Ru, Co
Zinc (Zn)	206.200	Sb, Ta, Bi, Os

†Available from: http://www.esslab.com/iv/tech/periodic.html.

Instrument drift, which was calculated as the percent difference between standard runs, was within ± 10% for all standards greater than 10 µg/L. Antimony and Cu standards with concentrations less than 10 µg/L did not fall within ± 10%. This observed drift in low concentration standards will be taken into account in the discussion of tissue samples containing Sb and Cu.

The ICP-OES calibration curves were linear from 0–500 µg/L for Ba, Cu, Fe, and Zn and 0–10,000 µg/L for Sb and Pb. Sensitivity, experimental detection limits, and theoretical detection limits for the instrument are shown in Table 4.2. Barium had the highest sensitivity and lowest experimental limit of detection (LOD), which was a result of the high intensity ionic emission line. The high intensity of the 455.403 nm emission line also resulted in high background signals for Ba standards, which caused quantitation of some samples to fall below zero. Antimony was shown to have the lowest sensitivity and the highest experimental LOD of all the elements analyzed by ICP-OES. Antimony and Ba also had the lowest and highest theoretical LODs, respectively. The experimental LODs for each element were greater than the theoretical LOD indicating the experimental conditions were not optimal. Since LODs were calculated from the blank standards, the higher LODs were likely a consequence of laboratory procedures that were not performed in a ‘clean lab’ setting and standards that were not newly purchased.

Table 4.2 ICP-OES experimental and theoretical analytical figures of merit for each element spectral emission line studied

Element-Emission Line (nm)	Sensitivity ($I/\mu g\ L^{-1}$)	Limit of Detection ($\mu g\ L^{-1}$)	Varian 710-ES Axial Limit of Detection† ($\mu g\ L^{-1}$)
Pb-220	1.426 ± 0.003	3.77	1.5
Sb-206	0.397 ± 0.001	17.61	3
Ba-455	571 ± 4	0.10	0.03
Cu-327	20.31 ± 0.06	1.96	0.5
Fe-238	24.8 ± 0.1	1.09	0.2
Zn-206	2.07 ± 0.01	2.02	0.2

†Available from: http://iconsteel.net/images/Varian_710_Specifications.pdf.

In addition to a high experimental LOD, the three replicates of the lowest calibration standards (0, 10, and 25 µg/L) for Sb had relative standard deviations (RSD) greater than 15%. The uncertainty in the calibration of Sb will be taken into account in the discussion of tissue samples with Sb concentrations below 50 µg/L. The lowest standard concentrations of Pb and Cu also had RSDs above 15%. The quality of Pb calibration will be discussed for the quantitation of FJ samples with lower Pb concentrations, while the effect of the Cu calibration will be discussed for NJ samples with inherently lower Cu concentrations. Barium was the only element for which all standards had RSDs below 10%. The quality of calibration for low concentrations of Fe and Zn was similar to Pb and Cu, which was previously mentioned. Although the calibration for Fe and Zn was adequate for reliable quantitation above 5 µg/L, the concentration differences between GSR tissue samples and control tissue samples were not distinctive enough to allow differentiation of shot from unshot tissue and therefore, these two elements could not be used to assess differences in bullet type or firing distance. Control tissue containing increased concentrations of Fe and Zn was likely a result of inherent Fe and Zn in muscles and organs, as well as blood concentrating in the tissue during decomposition. In a study by Wunnapuk *et al.*, Fe and Zn were detected in control tissue from gunshot victims which in some samples were shown to be higher than concentrations in shot tissue.[6] As a result of the elevated concentrations of Fe and Zn in control tissue, these elements were excluded from further analysis.

The focus of the fresh tissue study was to assess the elements detected above LODs and above levels in the control samples, as well as to compare elemental concentrations between bullet types and between firing distances. A comparison of element concentrations, which were normalized to the mass of tissue digested, in GSR tissue samples and control tissue samples is

depicted in the bar plots in Figure 4.6. The elements detected above LODs and control samples in both NJ and FJ samples were Pb, Sb, and Ba. In addition to those three elements, Cu was also detected in FJ samples at concentrations above the LOD and control samples. Lead concentrations in GSR tissue samples were calculated to be significantly greater than control tissue samples at the 99% (or greater) confidence interval for both bullet types and firing distances as determined by a two-tailed Student's t-test. Antimony concentrations were determined to be significantly greater in GSR tissue samples at the 95% (or greater) confidence with the exception of the Sb concentration in the tissue shot with FJ ammunition at 5 cm. The Sb concentration for FJ 5 cm was only significantly greater than the control sample at the 80% confidence interval (Fig. 4.6C). The case for Ba and Cu differs from the other elements shown in Figure 4.6 as the control sample concentrations were quantified as negative values. Although Ba concentrations in control tissue were less than zero, the concentrations in fresh GSR tissue samples were greater than calculated LODs for all bullet types and firing distances. Copper concentrations in GSR tissue samples are not shown in Figures 4.6A or 4.6B since they were below calculated LODs for NJ samples.

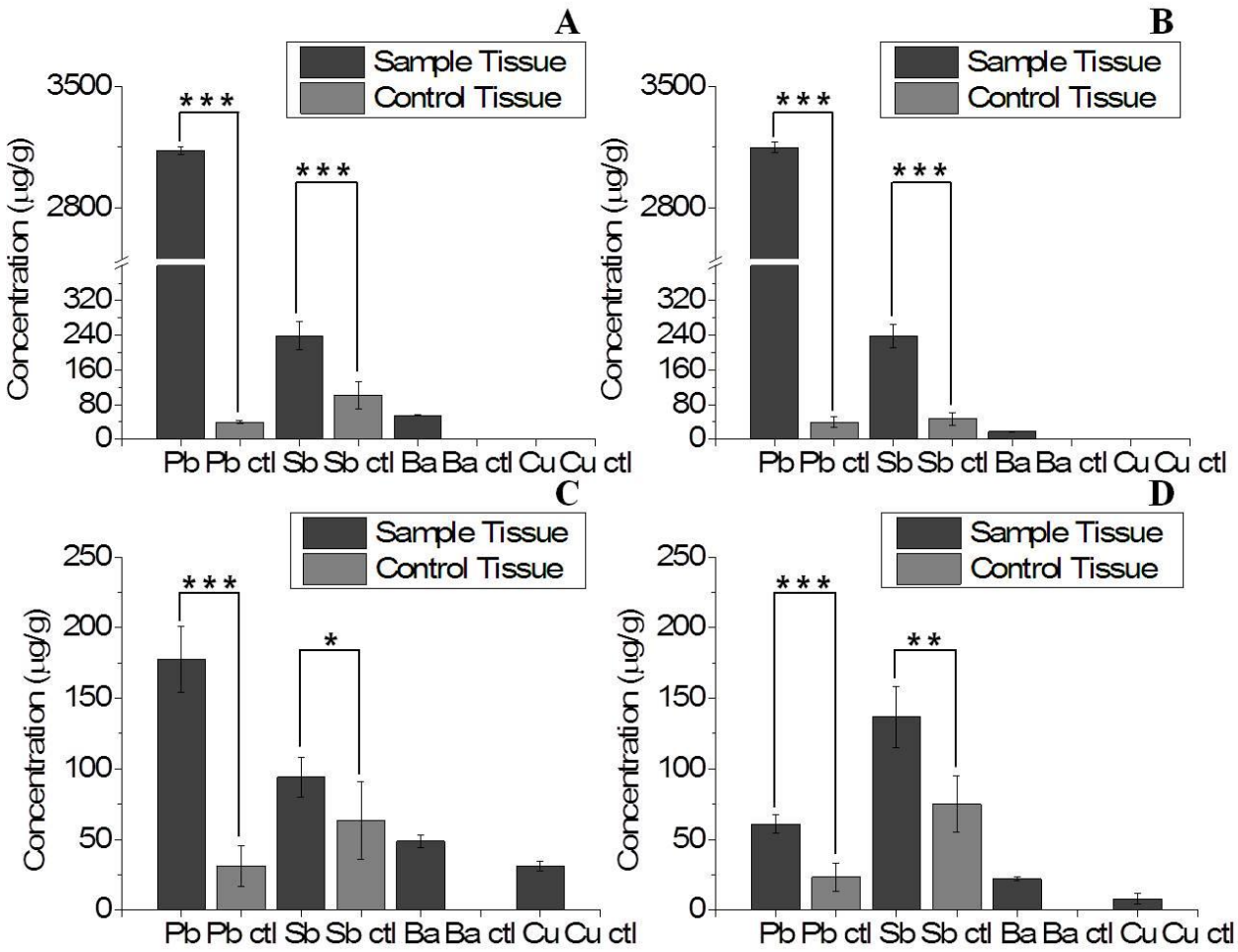

Figure 4.6 Gunshot residue tissue sample and control sample element concentrations (µg element/g tissue) determined by ICP-OES for (A) non-jacketed (NJ) samples shot at 5 cm, (B) NJ samples shot at 10 cm, (C) full-jacketed (FJ) samples shot at 5 cm, and (D) FJ samples shot at 10 cm. All concentrations are ± 1 standard deviation. Significant differences between mean concentrations are indicated with asterisks, where (***) indicates the 99% or greater, (**) 95%, and (*) 90% or lower.

As the concentrations of Pb, Sb, and Ba were above that of the LODs and control samples for both bullet types, Student's t-tests were used to determine significant differences between mean element concentrations from samples shot with different bullet types at the same firing distance and vice versa. The mean concentrations (±1 standard deviation) for Pb, Sb, Ba, and Cu in GSR tissue samples shot at 5 and 10 cm firing distances are shown in Table 4.3.

The corresponding plots comparing bullet type at 5 and 10 cm (Fig. 4.7A and B) indicate the level of significance attributed to the difference in each mean concentration based on the calculated t-statistic. At the 5 cm firing distance, element concentrations for Pb, Sb, and Ba were all significantly greater in NJ samples compared to FJ samples; however, the concentrations for Pb and Sb in NJ versus FJ samples were significantly different at a higher confidence level than for Ba (99% vs 90%). The greater difference observed for Pb and Sb between bullet types compared to Ba was due in part to the origins of each element. In NJ ammunition, Pb and Sb were present in both the lead bullet and the primer, whereas Ba was only present in the primer. In addition, the copper jacket covering the lead bullet in FJ ammunition suppresses the amount of Pb deposited in the firearm barrel and consequently causes a decrease in Pb concentrations in GSR deposited with FJ ammunition.[7] This was evident when comparing the Pb concentrations in NJ and FJ samples at both 5 cm and 10 cm shown in Figure 4.7A and 4.7B, respectively. The NJ-to-FJ ratios for Pb were 18 and 52 at 5 cm and 10 cm, respectively. In a study by Udey *et al*., an NJ-to-FJ Pb ratio of 12 was obtained by using ICP-MS for 5 cm firing distance samples despite the use of different primers.[8] This ratio is comparable to the NJ-to-FJ ratio of 18 obtained in this study using ICP-OES for 5 cm samples. A constant NJ-to-FJ ratio is not specifically of evidentiary value, but provides evidence of consistency in amount of Pb deposited by NJ and FJ bullet types between studies.

Table 4.3 Fresh tissue element concentrations from ICP-OES analysis of non-jacketed (NJ) and full-jacketed (FJ) tissue samples

Bullet Type (Firing Distance)	Element Concentration (µg element/g tissue)*			
	Pb-220	Sb-206	Ba-455	Cu-327
NJ (5 cm)	3130±21	238±33	55.1±0.4	-
NJ (10 cm)	3147±31	238±27	17.2±0.4	-
FJ (5 cm)	176±23	94±14	49±4	31±3
FJ (10 cm)	61±6	137±22	22±1	8±4

*±1 standard deviation (σ)

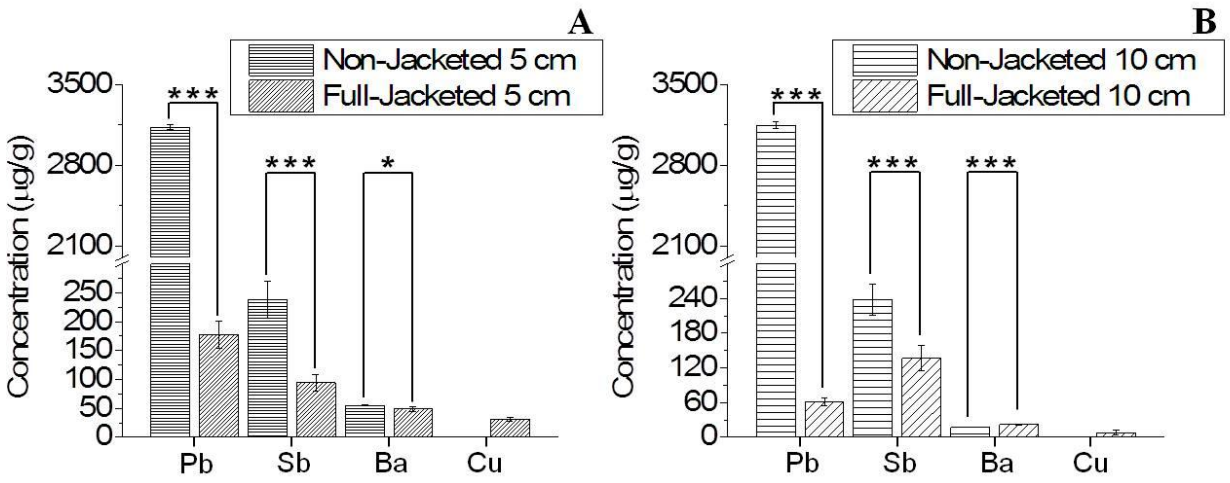

Figure 4.7 Comparison of bullet type using ICP-OES derived elemental concentrations (µg element/g tissue) of lead (Pb), antimony (Sb), barium (Ba), and copper (Cu) from samples shot at (A) 5 cm and (B) 10 cm. Significant differences between mean concentrations are indicated with asterisks, where (***) indicates the 99% or greater, (**) 95%, and (*) 90% or lower.

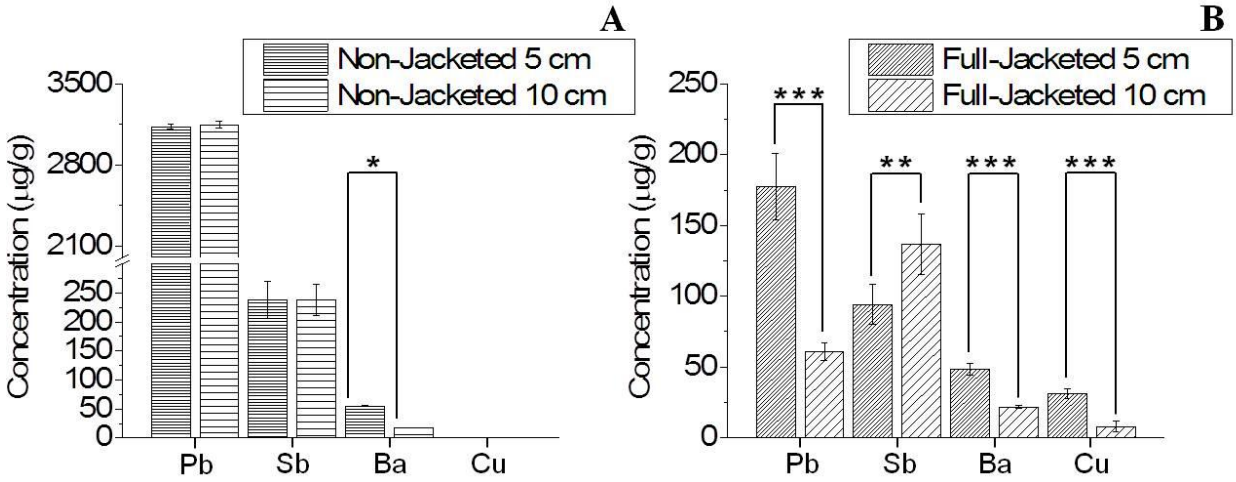

Figure 4.8 Comparison of firing distance using ICP-OES derived elemental concentrations (µg element/g tissue) of lead (Pb), antimony (Sb), barium (Ba), and copper (Cu) from samples shot with (A) non-jacketed and (B) full-jacketed ammunition. Significant differences between mean concentrations are indicated with asterisks, where (***) indicates the 99% or greater, (**) 95%, and (*) 90% or lower.

The results from the bullet type comparison were similar for the 10 cm firing distance, with the exception of Ba as shown in Figure 4.7B. Pb and Sb were again significantly greater in NJ samples than in FJ samples, whereas Ba was significantly greater in the FJ sample at a 10 cm firing distance. The significant differences in concentration observed for Pb and Sb between NJ and FJ samples suggest that these elements were useful in the differentiation of bullet type in fresh tissue. Barium concentrations in NJ and FJ samples, although significantly different, cannot be used to differentiate bullet type since Ba was not higher for one bullet type at both firing distances.

Another distinguishing factor used to differentiate FJ samples from NJ samples was elevated Cu concentrations. As mentioned previously, Cu was not detected above LODs in NJ samples, but Cu was present in quantifiable amounts in FJ samples. The sole source of Cu in NJ samples was the brass cartridge case, whereas FJ samples had multiple sources of Cu with the major contribution from the copper jacket coating the bullet.

The mean element concentrations for the firing distance comparison are shown in Figure 4.8. For the NJ samples, the mean concentrations of Pb and Sb were similar for both firing distances and were not significantly greater in 5 cm samples compared to those with GSR deposited from 10 cm; however, the Ba concentration was significantly greater in 5 cm samples compared to 10 cm at the 90% confidence interval (Fig. 4.8A). The amount of GSR deposited close to the entry wounds for the NJ 5 cm and NJ 10 cm pigs was visually similar (Fig. 4.1A and B) in contrast to the amount of GSR deposited a few centimeters from the entry wound. Since the tissue samples were excised directly adjacent to the entry wound, finding similar concentrations of the major components of GSR was not surprising.

Student's t-tests performed for all Pb, Sb, Ba, and Cu concentrations in FJ tissue samples indicated significant difference in concentration for 5 and 10 cm firing distances for all four elements (Fig. 4.8B). The mean concentrations of Pb, Ba, and Cu were significantly different in 5 cm samples compared to 10 cm at the 99% confidence interval and at the 95% confidence interval for Sb. Lead, Ba, and Cu concentrations were all greater in samples shot at 5 cm as expected, while Sb had significantly higher concentrations in the FJ sample shot at a 10 cm distance (Fig. 4.8B). Since Pb and Sb originate from the same sources in the firearm cartridge, it follows that the Pb-to-Sb ratio should remain constant. The Pb-to-Sb ratio was not maintained in the FJ samples indicating that the higher Sb concentration in the FJ 10 cm sample was possibly the result of a sampling and/or quantitation error. A more detailed discussion on sources of error is presented in the next section.

4.2.2 ICP-MS Analysis of Fresh Tissue Samples

The fresh tissues samples from Day 0 were also analyzed by ICP-MS. The ICP-MS results differ from the ICP-OES results in that no replicate measurements were obtained. As a consequence, the ICP-MS results will be discussed with a focus on the detection of elements at concentrations above the limit of quantitation (LOQ), which was determined to be the lowest linear concentration on the calibration curve. As was done with the ICP-OES analysis, the quality of the calibration and analytical figures of merit were assessed for the ICP-MS instrument. The isotopes selected for each element are indicated for Pb, Sb, Ba, and Cu in Table 4.4 along with the sensitivities of the calibration, LOQs, and the theoretical LODs provided by the manufacturer for the mass spectrometer. The element LOQs were used for the ICP-MS analysis since a LOD could not be calculated without replicate measurements. Iron and Zn were

excluded from this discussion due to the inability to differentiate Fe and Zn concentrations in shot tissue from unshot tissue collected as control samples.

ICP-MS calibration curves were linear in the range 0–500 µg/L for Ba and Cu and 0–10,000 µg/L for Sb and Pb. The LOQ for each element represents the lower limit of the linear range for element calibration. Barium had the highest LOQ and the lowest sensitivity of the six elements investigated, which was in contrast to the ICP-OES results. ICP-MS had lower background signals compared to ICP-OES which contributed to higher sensitivities and lower theoretical LODs. The higher LOQ for Ba was a result of the standard concentrations less than 5 µg/L not maintaining linearity with the higher concentration standards. Despite the higher LOQ for Ba, all of the element concentrations were quantified above the LOQ in both the fresh and decomposition samples.

Table 4.4 ICP-MS experimental and theoretical analytical figures of merit for each element isotope studied

Element	Sensitivity ($/10^{-4}$) ($I/\mu g\ L^{-1}$)	Limit of Quantitation ($\mu g\ L^{-1}$)	Agilent 7500 Series Limit of Detection† ($\mu g\ L^{-1}$)
^{208}Pb	27.72 ± 0.07	1	0.00040
^{121}Sb	12.11 ± 0.03	1	0.00021
^{137}Ba	3.06 ± 0.09	5	0.00038
^{65}Cu	21.96 ± 0.50	2.5	0.0278
^{56}Fe	16.63 ± 0.34	2.5	0.00503
^{66}Zn	4.75 ± 0.04	2.5	0.00161

†Available from: http://www.chem.agilent.com/Library/applications/5989-1041EN.pdf.

Elemental concentrations from the ICP-MS analysis are shown in Table 4.5. At the 5 cm firing distance, Pb, Sb, Ba, and Cu were detected in both NJ and FJ samples. This was an improvement from ICP-OES, where Cu was not detected in NJ samples. ICP-MS fresh tissue results comparing bullet type are shown in Figure 4.9. At 5 cm, Pb and Sb were greater in NJ samples, whereas Ba was comparable in both NJ and FJ samples. The similar Ba concentrations for NJ and FJ samples at 5 cm were in contrast to ICP-OES results which showed a significant difference between bullet types. The differences in element concentrations observed between ICP-OES and ICP-MS are discussed at the end of this section. Copper concentrations were greater in the FJ 5 cm sample by more than five times compared to the NJ 5 cm sample. This difference could not be assessed using the ICP-OES results as Cu was not detected above LODs in NJ samples. Similar results were obtained for the bullet type comparison at the 10 cm firing distance. As was observed for the ICP-OES results, Ba could not be used to differentiate bullet type, while Pb and Sb concentrations were different for both bullet types. Using ICP-MS, Cu had more discriminatory power compared to ICP-OES since it was detected for both bullet types.

As was observed for the ICP-OES results, Pb and Sb had comparable concentrations in NJ samples for both firing distances as shown in Figure 4.10. Ba had a higher concentration at the shorter firing distance in the NJ sample as expected. Copper concentrations were similar for both NJ firing distances. The firing distance comparison for the FJ samples showed all four elements were greater at the shorter firing distances. Since the Sb concentration was quantified to be greater in the FJ 5 cm sample by ICP-MS, an ICP-OES an error in the calibration of Sb and not a sampling error is likely the source of the opposite result that was observed in the ICP-OES analysis of Sb discussed previously.

Table 4.5 Fresh tissue element concentrations from ICP-MS analysis of non-jacketed (NJ) and full-jacketed (FJ) tissue samples

Bullet Type (Firing Distance)	Element Concentration (µg element/g tissue)‡			
	^{208}Pb	^{121}Sb	^{137}Ba	^{65}Cu
NJ (5 cm)	1912	134	45	3
NJ (10 cm)	1959	120	21	3
FJ (5 cm)	115	33	45	25
FJ (10 cm)	31	18	25	8

‡No standard deviation reported for one concentration measurement

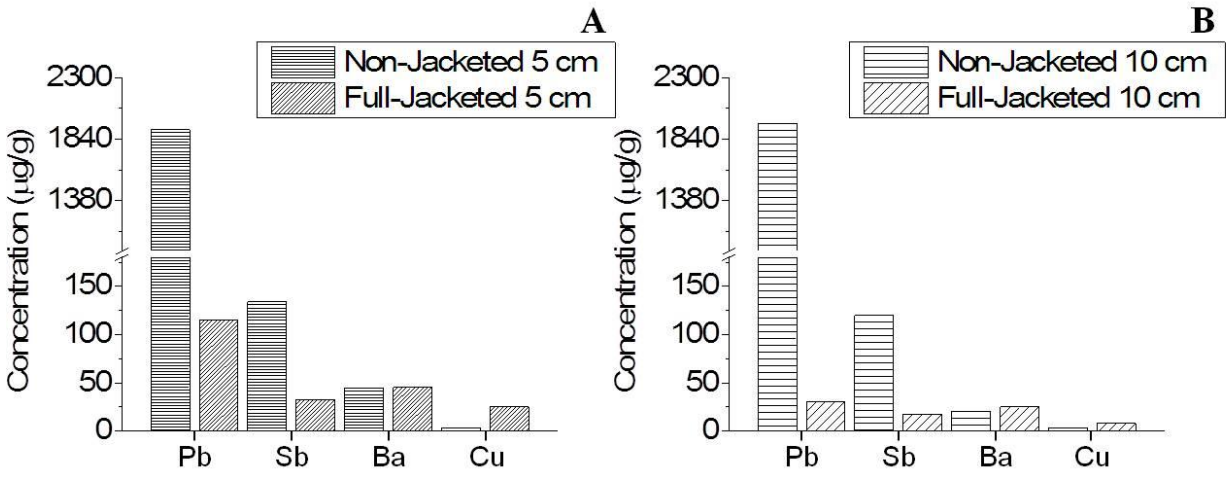

Figure 4.9 Comparison of bullet type using ICP-MS derived elemental concentrations (µg element/g tissue) of lead (Pb), antimony (Sb), barium (Ba), and copper (Cu) from samples shot at (A) 5 cm and (B) 10 cm. Bar plots represent one concentration measurement.

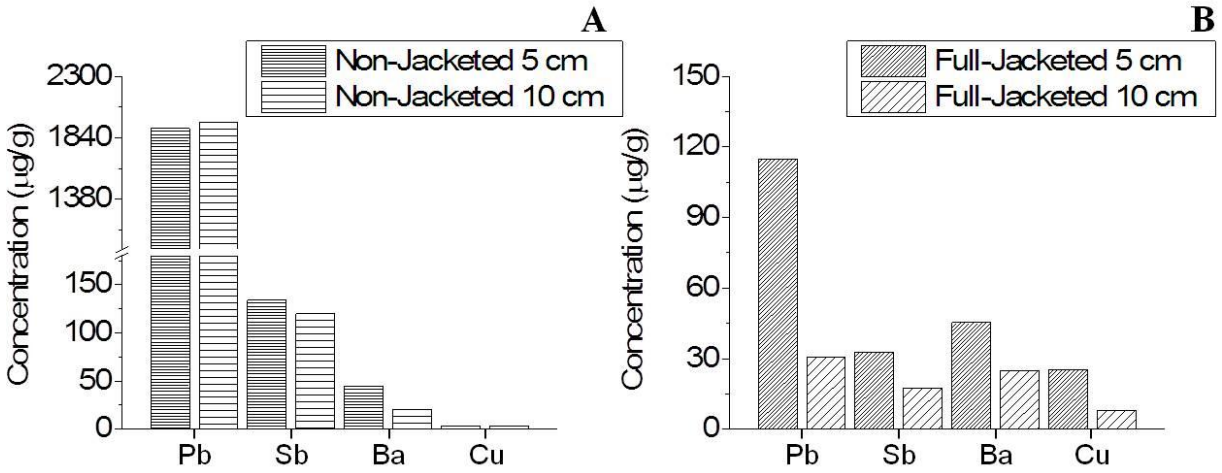

Figure 4.10 Comparison of firing distance using ICP-MS derived elemental concentrations (µg element/g tissue) of lead (Pb), antimony (Sb), barium (Ba), and copper (Cu) from samples shot with (A) non-jacketed and (B) full-jacketed ammunition. Bar plots represent one concentration measurement.

A comparison of the ICP-OES and ICP-MS data (Tables 4.3 and 4.5) showed discrepancies in element concentrations between the two analytical techniques. The OES-to-MS concentration ratios were greater than one for all Pb and Sb samples, while they were less than one for Ba samples shot at 10 cm (Table 4.6). A systematic error in one analysis technique would most likely result in a constant ratio either greater or less than one for all samples. The OES-to-MS ratios observed in the fresh tissue data were observed to vary according to element, as well as bullet type and firing distance. In examining the whole data set, including the decomposition samples described in the next section, a few conclusions were drawn. The best agreement between analyses was determined by the samples with OES-to-MS ratios closest to one. For Pb, the best agreement was observed for NJ samples, while a majority of FJ samples had ratios greater than two. The best agreement for Sb was also observed in NJ samples; however, Sb had the worst agreement overall with some sample ratios greater than five. A majority of Ba OES-to-MS ratios were less than two and most of the FJ ratios less than one. The best agreement for Ba was observed in NJ 5 cm samples. Copper concentrations in FJ samples analyzed by ICP-OES had good agreement with ICP-MS as shown by the ratios close to one for both firing distances. The discrepancies between analysis techniques were most likely the result of differences in instrumental sensitivity which varied for each element. This was particularly noticeable in the case of Sb, which had low sensitivity in the ICP-OES analysis and relatively high sensitivity for the ICP-MS analysis.

Table 4.6 Elemental concentration ratios (OES/MS) for non-jacketed (NJ) and full-jacketed (FJ) fresh tissue samples

Bullet Type (Firing Distance)	ICP-OES-to-ICP-MS Element Concentration Ratio			
	Pb	Sb	Ba	Cu
NJ (5 cm)	1.64	1.77	1.24	-
NJ (10 cm)	1.61	1.98	0.827	-
FJ (5 cm)	1.54	2.88	1.07	1.24
FJ (10 cm)	1.99	7.82	0.878	0.997

Although there was no constant OES-to-MS ratio observed for any one element, there were some apparent trends in the NJ-to-FJ ratios. As stated previously, the NJ-to-FJ ratios may not be of evidentiary value, but the ratios were used here to verify the consistency of the results from the two analytical techniques despite the difference in quantitation. An inspection of Figures 4.7 and 4.9, which depict NJ and FJ concentrations in bar plots for ICP-OES and ICP-MS results, respectively, showed similar trends, but the concentrations were on different scales. To assess these trends, the NJ-to-FJ ratios were calculated for ICP-OES and ICP-MS results at 5 and 10 cm. The ratios for Ba and Cu (ICP-MS only) were consistent, which indicated good agreement between analyses. On the other hand, the ratios for Pb and Sb had higher magnitudes and wider ranges. Since the same primer was used for both types of ammunition, the greater magnitudes were attributed to the difference in NJ and FJ bullet composition, whereas the spread in NJ-to-FJ ratios for Pb and Sb were likely due to instrumental sensitivity and calibration. A comparison of ICP-OES and ICP-MS quantitation requires a reassessment of the figures of merit for Pb and Sb (Tables 4.2 and 4.4). The differences in sensitivity for Sb stated previously would explain the spread in Sb, while the spread in NJ-to-FJ ratio for Pb manifested as a result of the high concentrations that were close to the maximum of the linear range of the calibration curve. Based on these results, the disagreement between ICP-OES and ICP-MS concentrations were not attributed to a systematic error in the ICP-OES instrument; however, the issues in quantitation of some elements by ICP-OES stated above would need to be addressed in order to achieve absolute agreement. ICP-OES instrumental accuracy would have been improved by use of internal standards and a narrower standard concentration range.

4.2.3 Fresh Tissue Summary

The fresh tissue ICP-OES analysis showed Pb, Sb, and Ba were detected above control samples in samples shot with both bullet types, while Cu was detected above controls in samples shot with FJ ammunition. Lead and Sb were useful for bullet type differentiation as both elements had significantly higher concentrations in NJ samples. Barium was used to differentiate firing distance for both bullet types and Cu concentrations were used in differentiation of firing distance for FJ samples only. The ICP-MS analysis verified the ICP-OES results in that Pb and Sb had higher concentrations in NJ samples at both firing distances and Ba had higher concentrations at the shorter firing distance. ICP-MS was used to quantitate Cu in both NJ and FJ samples and showed Cu had higher concentrations in FJ samples. The direct comparison of elemental concentrations determined by both techniques showed discrepancies. Those differences were associated with differences in sensitivity for individual elements between ICP-OES and ICP-MS and not a systematic error in one technique.

4.3 Decomposition Tissue Studies

The twenty tissue samples collected throughout decomposition from one through 26 days after death were prepared as described in section 3.2 and analyzed by ICP-OES and ICP-MS. Previous studies have shown ICP-MS was successful in detecting Pb, Sb, and Ba during both moderate and advanced decomposition.[8, 9] In the present study, the objective was to assess ICP-OES, a relatively inexpensive and widely available technique, in the detection the Pb, Sb, Ba, and Cu during decomposition.

4.3.1 ICP-OES Analysis of Decomposed Tissue Samples

The GSR tissue samples collected throughout decomposition were first assessed on whether Pb, Sb, and Ba were detected. Elemental concentrations were plotted as a function of

time since death (in days) for each combination of bullet type and firing distance (Fig. 4.11A-D). Lead had the greatest concentration of the three primer elements followed by Sb and then Ba. This trend persisted throughout decomposition in NJ samples, but Pb was not always greater than Sb in FJ samples. For the NJ 5 cm sample, all three elements were detected through 12 days of decomposition (Fig. 4.11A). Lead was detected in all five NJ 5 cm decomposition samples. The persistence of Pb on the gunshot wounds was likely due to the high concentrations deposited on Day 0 (3130 ± 20 µg/g) with the NJ ammunition at close range. There was an overall decrease in concentration for Pb, Sb, and Ba over the period of sample collection, while there were some variations in concentration from sample to sample. Lead concentration, shown in Figure 4.11A, for example, increased from 9054 ± 40 µg/g on Day 1 to 12323 ± 31 µg/g on Day 5 and then decreased again to 4667 ± 24 µg/g on Day 7. These variations could be the result of separate shots collected from different physical locations on the carcass, sampling inconsistencies when sections of the wounds were prepared for digestion, pipetting errors during sample preparation and/or quantitation errors. Any errors occurring during sample collection or preparation, such as sampling inconsistencies occurring during the dissection of the wounds prior to microwave digestion, would also affect the ICP-MS results and sample to sample variations would be observed since the same digests were used for both analyses. The ICP-MS results presented in the next section showed that not all of the increases and decreases coincide between ICP-OES and ICP-MS, therefore it is likely the same quantitation errors discussed for Pb and Sb in the fresh tissue study also caused the observed sample to sample variations over time.

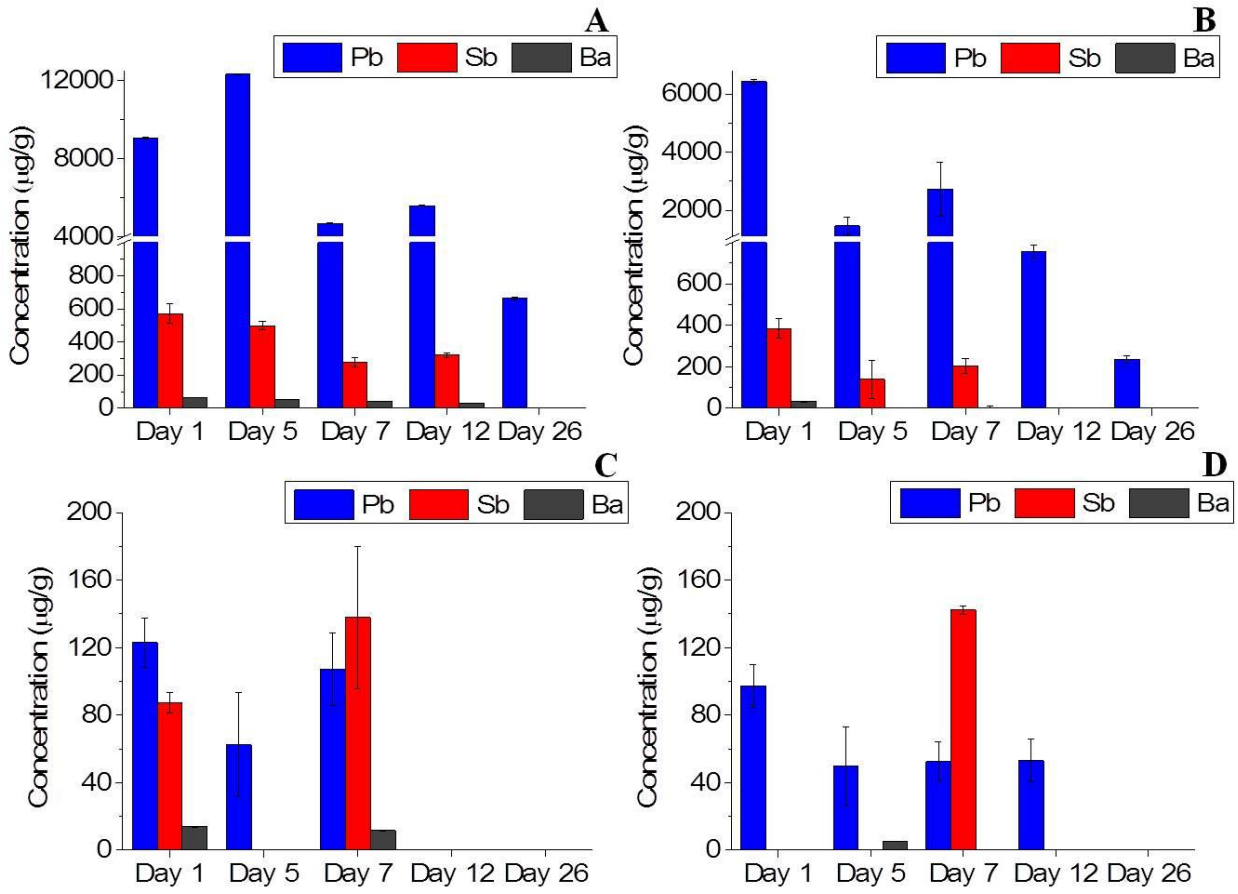

Figure 4.11 Elemental concentrations (µg element/g tissue) of lead (Pb) (blue), antimony (Sb) (red), and barium (Ba) (dark gray) from ICP-OES analysis of (A) non-jacketed (NJ) 5 cm, (B) NJ 10 cm, (C) full-jacketed (FJ) 5 cm, and (D) FJ 10 cm tissue samples. Time since death is shown on the x-axis. Concentrations less than LODs, control samples, and procedural blanks were omitted. Error bars represent ± 1 standard deviation.

As was observed for NJ 5 cm samples, Pb was detected throughout decomposition in NJ 10 cm samples, whereas Sb and Ba were not detected beyond Day 7 in NJ 10 cm samples (Fig. 4.11B). Lead concentrations in NJ 10 cm samples decreased from 6428 ± 71 µg/g on Day 1 to 235 ± 16 µg/g on Day 26. Antimony and Ba decreased by a smaller amount between Day 1 and Day 7 with differences of 181 µg/g and 28 µg/g, respectively. From an evidentiary standpoint, a confirmation of GSR based on the presence of all three elements could only be made for Day 1 and Day 7. On Day 7, this confirmation was tentative due to the low concentration of Ba and the uncertainty associated with the Sb ICP-OES standard calibration. In a study by Wolten *et al*., criteria for GSR identification were established based on the elemental composition of GSR particles on shooter's hands.[10] The compositional criteria listed the combinations of Pb, Sb, and Ba, as well as the combination of Sb and Ba as characteristic of GSR, while the presence of Pb and Sb, Pb and Ba or only Pb were labeled consistent with GSR. Using these criteria as a benchmark, the combination of Pb and Sb observed on Day 5 in the NJ 10 cm sample was consistent with GSR as were the samples from Days 12 and 26 containing Pb. The elements originating in the bullet and the primer were highest in NJ samples, which made detection via ICP-OES possible early in the study.

The FJ samples which contained lower concentrations of Pb, Sb, and Ba highlight the limitations of ICP-OES for GSR analysis during decomposition. As shown in Figure 4.11C-D, Pb was only detected through seven days of decomposition in FJ 5 cm samples and through 12 days in FJ 10 cm samples. The concentration of Pb decreased from 123 ± 15 µg/g to 107 ± 21 µg/g in FJ 5 cm samples from Day 1 to Day 7. Even though the decrease in Pb concentration from Day 1 to Day 7 was not great, the concentrations on Day 12 and Day 26 were lower than procedural blanks indicating that ICP-OES had a high background limiting the detection

capabilities for the decomposition samples. FJ 5 cm samples showed two days in which all three elements were present although the low concentrations of Ba and the high uncertainty of Sb make these data suspect. In the FJ 10 cm samples, all three elements were not detected in the same wound.

Student's t-tests were used to identify significant difference in mean element concentrations in order to differentiate bullet type and firing distance. Bullet type was differentiated at the 5 cm firing distance using Pb, Sb, and Ba on Day 1. Each element concentration was significantly greater in NJ samples at the 99% (or greater) confidence interval. In addition, Pb was significantly greater in NJ samples compared to FJ samples on Days 5 and 7 (99%), while Sb was significantly different on Day 7 (99%). At the 10 cm firing distance, bullet type was differentiated using Pb on Days 1 through 12 (99%), while Sb was significantly different on Day 7 at the 95% confidence interval.

Lead was the most useful for firing distance differentiation for NJ samples during decomposition. Lead was significantly greater in NJ 5 cm samples compared to 10 cm samples on Days 1, 5, 12 and 26 at 99% confidence and Day 7 at 95% confidence. Antimony was significantly greater in NJ 5 cm samples on Day 5 at 99% confidence and Days 1 and 7 at 95% confidence.

The low element concentrations in FJ samples made differentiating firing distance difficult. Lead concentration was significantly greater in 5 cm samples at 95% confidence than 10 cm samples on Day 7 and 90% confidence on Day 1, while Sb and Ba were either not detected in the same wound or not significantly different between firing distances.

In section 4.2.1, it was noted that Cu concentrations were lower than the LOD in NJ samples. This was also observed for samples collected during decomposition, but Cu was

detected above the LOD in FJ samples. Copper concentrations in FJ samples are shown in Figure 4.12 as a function of time since death (in days). These results showed that even though Cu was detected in FJ samples, the concentrations over time were variable and not useful in differentiating firing distance beyond Day 1. The concentration of Cu was significantly greater in the 5 cm sample on Day 1 at a 95% confidence interval. On Day 26, Cu was significantly greater in the 10 cm sample, although the concentration was unexpectedly high. As will be shown in the next section, ICP-MS analysis of Cu also showed a high concentration on Day 26 for the FJ 10 cm sample, which could be an indication of a sampling error.

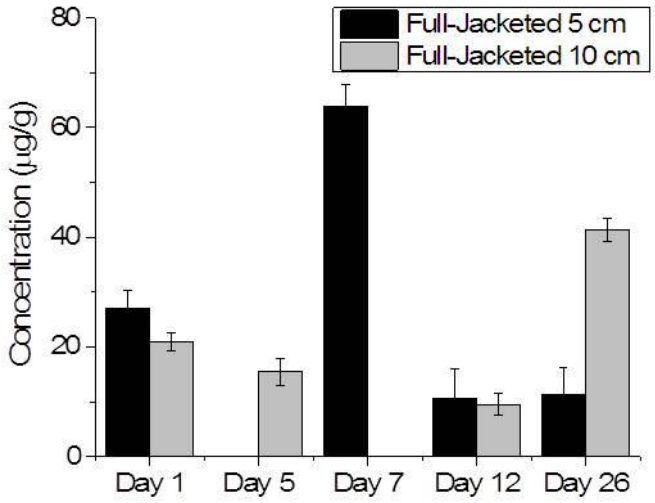

Figure 4.12 Elemental concentrations (µg element/g tissue) of copper (Cu) from ICP-OES analysis of FJ 5 cm (black) and FJ 10 cm (gray) samples. Time since death shown on x-axis. Concentrations less than LODs, control samples, and procedural blanks were omitted.

4.3.2 ICP-MS Analysis of Decomposed Tissue Samples

The ICP-MS analysis of the decomposition samples was intended to be a proof-of-concept in the context that similar analyses have been performed previously and this analysis was used as a comparison, as well as a validation of the ICP-OES results discussed in the previous section. There were no replicates for the ICP-MS analysis so there will be a discussion of the results without strenuous statistical comparisons. As was the case for ICP-OES decomposition results, ICP-MS elemental concentrations were plotted as a function of time since death (in days) for each combination of bullet type and firing distance (Fig. 4.13A-D). For all NJ samples, Pb, Sb, and Ba were all detected throughout decomposition. All concentrations were above documented LOQs and were detected at higher concentrations than in control tissue. Barium concentrations were the lowest of the three characteristic elements and were detected in all samples even though the bar plots for NJ samples do not depict Ba on Day 26 due to the scale. The three primer elements were also detected through Day 26 in FJ samples, which highlights the greater sensitivity of ICP-MS when compared to ICP-OES, as these elements were not detected in FJ samples throughout decomposition by ICP-OES. During decomposition, there was an apparent trend in Pb and Sb concentrations decreasing at the same rate which is discussed in more detail below.

Although t-tests were not performed on the ICP-MS data due to lack of replicates, concentration differences were observed between NJ and FJ samples, as well as between firing distances of 5 cm and 10 cm. Lead concentrations were consistently greater in NJ samples compared to FJ samples at both firing distances throughout decomposition. The difference between NJ and FJ 5 cm Pb concentrations ranged from over 5000 µg/g on Day 1 to 398 µg/g on Day 26. Antimony was also consistently greater in NJ samples at both firing distances; however,

the concentration differences were not as stark as was observed for Pb. The concentration differences between bullet types for Sb in 5 cm samples ranged from 304 µg/g on Day 1 to 17 µg/g on Day 26. Barium had consistently higher concentrations in NJ samples at 5 cm, but not in all 10 cm samples. After Day 5, the Ba concentrations were comparable between the two bullet types and did not allow discrimination. The large concentration differences observed for Pb during decomposition point to its utility in discriminating bullet type during decomposition, whereas Sb and Ba were shown not to have as much value as Pb for this purpose.

In comparing firing distances of the NJ bullet type, the difference in Pb concentration between 5 cm and 10 cm ranged from 1751 µg/g on Day 1 to 288 µg/g on Day 26. These concentration differences indicated Pb could be useful in differentiating firing distance during decomposition; however, Pb did not consistently have a higher concentration at 5 cm in all NJ samples. The same was true for Sb concentrations in NJ samples, where the 10 cm sample had a higher concentration compared to the 5 cm sample on Day 7. Barium concentrations were consistently higher in NJ 5 cm samples compared to 10 cm with concentration differences ranging from 24.7 µg/g on Day 1 to 2.3 µg/g on Day 26 indicating some discrimination in firing distance was possible using Ba. For firing distance comparison in FJ samples, the concentration differences were lower for Pb, Sb, and Ba and were not consistently greater in 5 cm samples. Barium, which was used to discriminate, firing distance in NJ samples, had the greatest concentration difference between 5 and 10 cm in FJ samples on Day 7. Days 12 and 26 had higher Ba concentrations in 10 cm samples compared to 5 cm samples. In this case, the variable condition of the decomposed tissue may have affected the results. The FJ 5 cm pig was at a later stage of decomposition compared to the FJ 10 cm pig, which was at a stage of advanced decay on Day 26. Lead and Sb concentrations were also affected by the variable decomposition as both

had higher concentrations in the FJ 5 cm samples compared to 10 cm with the exception of Days 12 and 26. The three characteristic elements were able distinguish 5 cm samples from 10 cm samples through Day 7 at which time the differences in decomposition rate of the porcine tissue affect the elemental concentrations.

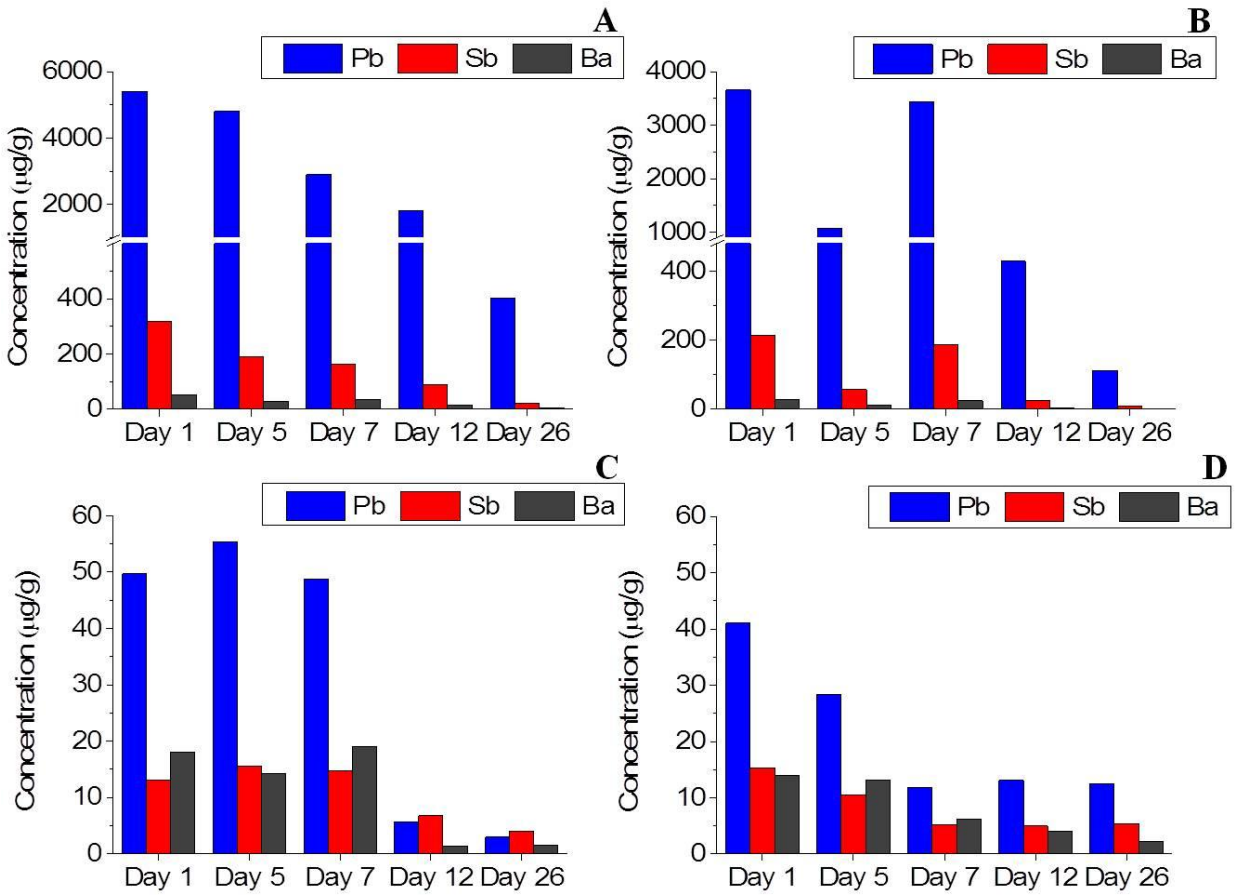

Figure 4.13 Elemental concentrations (µg element/g tissue) of lead (Pb) (blue), antimony (Sb) (red), and barium (Ba) (dark gray) from ICP-MS analysis of (A) non-jacketed (NJ) 5 cm, (B) NJ 10 cm, (C) full-jacketed (FJ) 5 cm, and (D) FJ 10 cm tissue samples. Time since death is shown on the x-axis. Bar plots represent one concentration measurement.

An interesting feature of the ICP-MS data was the apparent correlation between element concentrations. Plots of Sb vs Pb concentration in Figure 4.14 highlight this association. Pearson product-moment correlation (PPMC) coefficients were calculated between the elemental concentrations of Sb and Pb, Ba and Pb, as well as Ba and Sb for each combination of bullet type and firing distance (Table 4.7). The strongest positive correlation between Sb and Pb was observed for NJ 10 cm samples with a PPMC coefficient of 0.997. The other PPMC coefficients for Sb vs Pb were 0.986, 0.940, and 0.907 for FJ 5 cm, NJ 5 cm and FJ 10 cm, respectively. A correlation between these elements is not a defining factor in assessing the presence of GSR or discriminating between samples; however, a strong correlation (i.e., greater than 0.80) does strengthen the argument that these elements originate from the same sources within the ammunition cartridge and no contamination from external sources of Pb or Sb occurred. Within the NJ ammunition cartridge, Pb originated from the primer and the bullet. Antimony was also present in the primer formulation and present as a component of the metal alloy comprising the bullet. In the FJ cartridge, the bullet had a lead-antimony core and was coated with copper resulting in decreased amounts of Pb and Sb in the GSR deposited, but a strong correlation still existed due to the presence of both Pb and Sb in the primer.

Barium, which originated in the primer, had moderate correlation (i.e., correlation coefficients between 0.50 and 0.79) with Pb for NJ 5 cm and FJ 10 cm, while correlations for NJ 10 cm and FJ 5 cm were strong. Overall the correlation between Ba and Pb was not as strong as for Sb and Pb due to the fact that Ba was only present in primer and was not also present in the bullet. The association between Ba and Sb was expected to be similar to that of Ba and Pb; however Ba and Sb had stronger correlation compared to Ba and Pb indicating the strength of the linear association between Ba and Sb was unaffected by the contribution of Sb from the bullet.

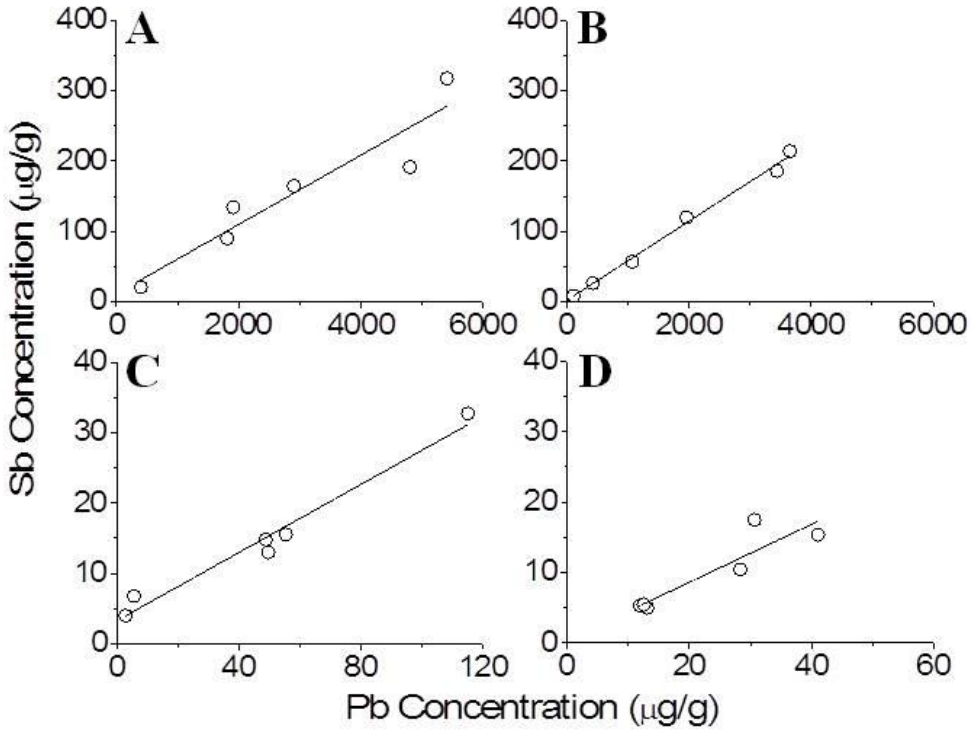

Figure 4.14 Plots of antimony (Sb) vs lead (Pb) concentrations (µg element/g tissue) from ICP-MS analysis of (A) non-jacketed (NJ) 5 cm, (B) NJ 10 cm, (C) full-jacketed (FJ) 5 cm, and (D) FJ 10 cm tissue samples from Day 0 through Day 26.

Table 4.7 Pearson product moment correlation (PPMC) coefficients showing linear correlation between element concentrations from six tissue samples analyzed by ICP-MS

Bullet Type (Firing Distance)	PPMC coefficient		
	Sb/Pb	Ba/Pb	Ba/Sb
NJ (5 cm)	0.940	0.701	0.859
NJ (10 cm)	0.997	0.969	0.977
FJ (5 cm)	0.986	0.983	0.982
FJ (10 cm)	0.907	0.750	0.937

PPMC coefficients provided a way to assess the correlation between elements, but were not able to provide any differentiation between bullet type or firing distance. Average element ratios were calculated in order to focus on the differences in element relationships for each combination of bullet type and firing distance (Table 4.8). The average ratios were calculated from the element concentrations in the six tissue samples collected in both the fresh and decomposition study.

The average element concentration ratios for Sb/Pb in NJ samples at 5 and 10 cm were within error of one another, which indicated that firing distance had no discernible effect on element ratios in GSR. There was also no statistical difference as determined by a Student's t-test at 80% confidence for Ba/Pb average concentration ratios when comparing NJ 5 cm and 10 cm samples. Comparing firing distance in the FJ samples, there was also no statistical difference at 80% confidence between the average element ratios for 5 and 10 cm. As the exact primer formulation and bullet composition were unknown, the magnitude of the ratios themselves were not able to be used to trace GSR back to a specific ammunition type; however, the differences in element ratios observed between the NJ and FJ samples were used to compare and discriminate the two bullet types. Average Sb/Pb ratios for FJ samples of 0.614 and 0.428 for 5 and 10 cm, respectively, were nearly an order of magnitude higher than the ratios calculated for NJ samples, which were 0.054 and 0.061 for 5 and 10 cm, respectively. These ratios were calculated to be significantly different at a 95% confidence level and the differences in average ratios reflect the contribution of Pb from the bullet in the NJ sample. The copper coating on the FJ bullet caused a decreased contribution of Pb in the GSR which resulted in a higher Sb/Pb concentration ratio in the FJ samples. The contribution of Sb from the NJ bullet was not confirmed by the Sb/Pb ratios alone, but the ratios Ba/Pb provided evidence of the presence of Sb in the NJ bullet. In the NJ

samples, the Ba/Pb ratios were lower than the Sb/Pb ratios. This difference was either the result of the presence of Sb, but not Ba, in the NJ bullet or simply a higher amount of Sb in the primer formulation.

In order to determine the contribution of Sb from the NJ bullet, a comparison of the Ba and Sb content in primer was assessed. As the FJ ammunition had a coated bullet, the average element concentration ratios for FJ samples gave the best indication of primer content. The average Ba/Sb ratios for FJ bullets were close to one indicating both elements had approximately equal concentrations in the primer. Both NJ and FJ ammunition cartridges were loaded with same primer, so the lower Ba/Sb ratios observed for the NJ samples compared to the FJ samples were a result of Sb content in the NJ bullet. Overall, the NJ samples had lower average element concentration ratios compared to FJ samples due to the contributions of Pb and Sb in the NJ bullet. These results provided a way to discriminate bullet type for a data that did not include replicate measurements.

Table 4.8 ICP-MS average concentration ratios from six tissue samples for each combination of bullet type and firing distance

Bullet Type (Firing Distance)	Average Concentration Ratio		
	Sb/Pb	Ba/Pb	Ba/Sb
NJ (5 cm)	0.054 ± 0.010	0.012 ± 0.006	0.211 ± 0.065
NJ (10 cm)	0.061 ± 0.008	0.010 ± 0.005	0.163 ± 0.054
FJ (5 cm)	0.614 ± 0.516	0.362 ± 0.099	0.929 ± 0.523
FJ (10 cm)	0.428 ± 0.077	0.438 ± 0.221	1.001 ± 0.368

In addition to detection of Pb, Sb, and Ba, the ICP-MS analysis was also successful in detecting Cu above LOQs and above levels in the control tissue, with the exception of the NJ 5 cm sample collected on Day 26, which was below the control. The Cu concentrations in FJ samples are shown in Figure 4.15. Copper concentrations did not follow the decreasing trend that was observed for Pb, Sb and Ba during decomposition as there were a few anomalous samples, such as the FJ 5 cm sample from Day 7 and the FJ 10 cm sample from Day 26. Similar elevated concentrations were observed for the ICP-OES analysis as seen in Figure 4.12, which were attributed to a possible error occurring during sample preparation. No other element concentrations showed similar elevated concentration on Days 7 and 26, which ruled out a problem with dilution during sample preparation. Contamination with an external source of Cu was the most probable explanation; however, only two of 20 GSR samples in the decomposition study were affected.

A comparison of bullet type showed FJ samples had higher Cu concentrations in all of the 5 cm samples collected during decomposition and in most of the samples shot at 10 cm indicating Cu from the full metal jacket persists over time. Firing distance comparison using Cu concentrations in NJ samples was not useful due to the low Cu concentrations, while FJ samples did not show much differentiation between firing distance with the exception of those anomalous elevated concentrations discussed previously.

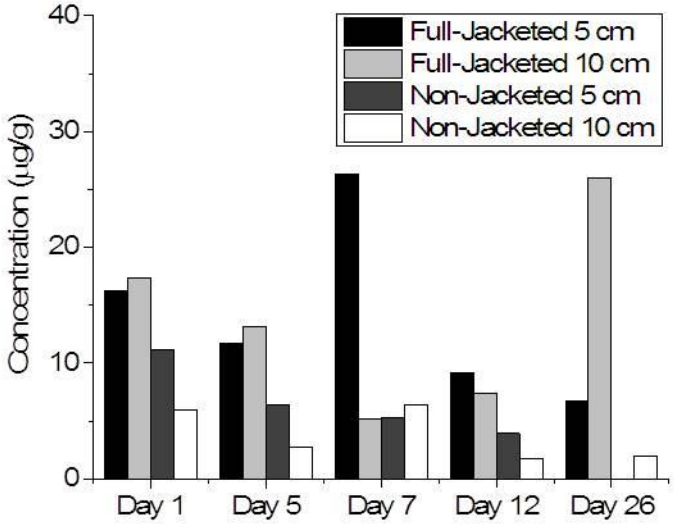

Figure 4.15 Elemental concentrations (µg/g) of copper (Cu) from ICP-MS analysis of full-jacketed (FJ) 5 cm (black), FJ 10 cm (light gray), non-jacketed (NJ) 5 cm (dark gray), and NJ 10 cm (white) samples. Time since death shown on x-axis. Bar plots represent one concentration measurement.

4.3.3 Decomposition Summary

In the ICP-OES of NJ samples, Pb was detected throughout decomposition, while Sb and Ba were detected through moderate decomposition (Day 12). Detection of Pb in multiple NJ and FJ samples collected during decomposition allowed for comparison and differentiation of bullet type, where Pb was determined to be significantly greater in NJ samples. The lower concentrations of Sb detected over time were not as reliable due to the low sensitivity in the ICP-OES analysis. A high sensitivity was determined for Ba; however, the lower initial concentrations and the high background from the ICP-OES made quantitation in the later stages of decomposition difficult. Copper was detected sporadically through decomposition, but the lower concentrations were not reliable due to the high RSDs in the low concentration standards.

In the ICP-MS analysis, Pb, Sb, and Ba were detected in both combinations of bullet type and firing distance throughout decomposition. Cu was also detected in FJ samples throughout decomposition and in NJ samples through 12 days of decomposition. No trend was observed that would allow differentiation of firing distance, but Cu concentrations were greater in FJ samples compared to NJ samples. There were correlations observed between elements concentrations originating in the NJ bullet and the primer in the fresh and decomposition samples. The correlations indicated both elements originated from the same sources in the ammunition. As further evidence of element origins in GSR, average element ratios confirmed the contribution of Sb from the NJ bullet. Average element ratios also were used to discriminate bullet type based on differences in element ratios between NJ and FJ samples.

REFERENCES

REFERENCES

1. Amendt J, Goff ML, Campobasso CP, Grassberger M, editors. Current concepts in forensic entomology. New York: Springer Science+Business Media B.V., 2010.

2. Rich J, Dean DE, Powers RH, editors. Forensic medicine of the lower extremity: Human identification and trauma analysis of the thigh, leg, and foot. Totown, NJ: Humana Press Inc., 2010.

3. Nelson DL, Cox MM. Lehinger principles of biochemistry. 5th ed. New York: W.H. Freeman and Company, 2008.

4. Wilson-Taylor RJ. Time since death estimation and bone weathering: The postmortem interval. In: Tersigni-Tarrant MA, Shirley NR, editors. Forensic anthropology: An introduction. Boca Raton, FL: CRC Press; 2013;339-80.

5. SWGGSR. Guide for primer gunshot residue analysis by scanning electron microscopy/energy dispersive x-ray spectrometry2011.

6. Wunnapuk K, Durongkadech P, Minami T, Ruangyuttikarn W, Tohno S, Vichairat K, et al. Differences in the element contents between gunshot entry wounds with full-jacketed bullet and lead bullet. Biol Trace Elem Res. 2007; 120:74-81.

7. Heard BJ. Handbook of firearms and ballistics. 2nd ed. Chichester, West Sussex, UK: John Wiley & Sons, Ltd, 2008.

8. Udey RN, Hunter BC, Smith RW. Differentiation of bullet type based on the analysis of gunshot residue using inductively coupled plasma mass spectrometry. J Forensic Sci. 2011; 56:1268-76.

9. LaGoo L, Schaeffer LS, Szymanski DW, Smith RW. Detection of gunshot residue in blowfly larvae and decomposing porcine tissue using inductively coupled plasma mass spectrometry (icp-ms). J Forensic Sci. 2010; 55:624-32.

10. Wolten GM, Nesbitt RS, Calloway AR, Loper GL, Jones PF. Particle analysis for the detection of gunshot residue. I: Scanning electron microscopy energy dispersive-x-ray characterization of hand deposits from firing. J Forensic Sci. 1979; 24:409-22.

Chapter 5: Conclusions and Future Directions

5.1 Conclusions

The objective of this research was to assess inductively coupled plasma-optical emission spectroscopy (ICP-OES) as a viable technique to detect gunshot residue (GSR) on both fresh and decomposed porcine tissue. Differentiation of bullet type and firing distance was evaluated using ICP-OES results from tissue samples shot with non-jacketed (NJ) and full-jacketed (FJ) ammunition at firing distances of 5 cm and 10 cm. The two combinations of bullet type and firing distance were also analyzed by inductively coupled plasma-mass spectrometry (ICP-MS) in order to evaluate the utility of both techniques in GSR detection with diminished elemental concentrations over a period of decomposition. ICP-OES has been studied as an attractive alternative to ICP-MS for use in forensic science laboratories due in part to lower capital and operating costs. Despite the cost effectiveness and greater accessibility of ICP-OES in forensic science laboratories, the inability of this technique to reach the low limits of detection accessed by ICP-MS made the technique inadequate to detect the persistence of all GSR elements in FJ samples over full decomposition. ICP-OES did prove a useful technique for the detection of GSR and discrimination of bullet type and firing distance in fresh tissue and in the detection of Pb in tissue shot with NJ ammunition during decomposition.

In the fresh tissue study, the characteristic elements of GSR, lead (Pb), antimony (Sb), and barium (Ba), were detected by ICP-OES at levels above those in control samples, procedural blanks, and limits of detection (LODs) in all NJ and FJ samples. In addition, Cu was detected in FJ samples at both firing distances. Iron (Fe) and zinc (Zn) had elevated concentrations in control tissue and as a result GSR tissue could not be differentiated from unshot tissue. Of the primer elements, Pb had the highest concentration in NJ samples due to its presence in both the primer

and the alloy composing the NJ bullet. The concentration of Pb in FJ samples was a factor of 10 lower than NJ samples, but was still a major component of the GSR. Copper concentrations in FJ samples were not nearly as high as the primer elements since the sources of Cu, including the full-metal jacket and the cartridge case, did not contribute high quantities to the GSR composition. Copper, unlike Sb and Ba, is more likely to be present in the environment so higher levels would be expected. As all the samples were exposed to the same external and laboratory environments, the presence of Cu in FJ and not NJ samples at detectable concentrations was taken to signify the origin of Cu as the full-metal jacket. Bullet type differentiation was achieved using Pb and Sb at confidence intervals of 99% or greater. Differentiating bullet type for both firing distances using two different elements was a significant result that provided confidence in the ability of ICP-OES to discriminate bullet type.

Barium was useful in differentiating firing distance for both bullet types, while Pb and Sb only differentiated firing distance for FJ samples. The Cu concentrations in FJ samples were also used to differentiate between 5 and 10 cm samples, while the mere presence of Cu in FJ samples was taken as a way to differentiate FJ from NJ bullet types. Based on this study, the differences in elemental concentration of the major component, Pb, between bullet types and the presence of a minor component, Cu, in FJ samples would be the most useful in a law enforcement investigation. Linking GSR to one bullet type would aid law enforcement in narrowing a suspect pool. Firing distance could not be determined using the methods in this study; however, the concentration differences of an element, such as Ba, could be used to determine if the multiple gunshot wounds were caused by shots fired from the same or different distances.

The ICP-MS analysis of GSR on fresh tissue samples verified the ICP-OES trends, but the analysis was not rigorous enough to provide statistical assessment. Differences in the ICP-MS and ICP-OES analyses manifested as differences in the absolute elemental concentrations. Lead and Sb concentrations showed the greatest differences in absolute concentrations. The OES-to-MS, as well as the NJ-to-FJ ratios were used to elucidate the causes of the discrepancies, which were ultimately determined to originate in the low sensitivity of ICP-OES for Sb and the proximity of Pb concentrations to the maximum limit of the linear range. Both techniques studied were successful in detecting the characteristic elements of GSR in fresh tissue; however, the limitations of ICP-OES became more apparent in the decomposition study.

In the ICP-OES analysis of tissue samples collected throughout decomposition, persistence of GSR was easier to assess in NJ samples due to the high quantity of residue deposited compared to FJ samples. Over the course of decomposition, the visible GSR deposited near the gunshot wound diminished, which made identification of the shot tissue difficult in some cases. The presence of elements commonly found in GSR on a wound observed on decomposing tissue provided confidence in the assumption that the wound was the result of a gunshot. In tissue shot with NJ ammunition, Pb was detected throughout decomposition, while Sb and Ba were detected through moderate decomposition. As Sb concentrations decreased, the confidence in accurate quantitation also decreased due to the relatively low precision in the low concentration Sb standards. Differentiation of bullet type and firing distance was possible in a few samples during decomposition despite the sporadic detection in FJ samples. Lead was used to differentiate bullet type in the first three decomposition samples at 5 cm and in the first four samples at 10 cm. Antimony concentrations could also be used to differentiate bullet type during

two days of decomposition in 5 cm samples and on one day in 10 cm samples. Barium successfully differentiated bullet type on the first day of decomposition in the 5 cm sample.

Firing distance determination in NJ samples was accomplished using Pb concentrations in all five samples collected throughout decomposition, Sb concentrations in the first three samples collected through Day 7, and Ba concentrations in the sample collected on the first day of decomposition. All of these elements had significantly greater concentrations in samples shot at 5 cm. Pb was the only element originating in primer used to differentiate firing distance in FJ samples. Copper was detected in FJ samples at either 5 cm or 10 cm throughout decomposition, but was not found to be useful in differentiation of bullet type or firing distance.

In the decomposition study, ICP-MS analysis was again used to verify the ICP-OES results and in this case of detecting the persistence of GSR, ICP-MS exceeded ICP-OES. ICP-MS detected Pb, Sb, and Ba in both combinations of bullet type and firing distance throughout decomposition. Cu was also detected in FJ samples throughout decomposition and in NJ samples through 12 days of decomposition. There were some differences in the sample to sample variation between ICP-OES and ICP-MS decomposition results and these differences were again attributed to instrumental sensitivity and calibration problems in ICP-OES. The ratios between the elements originating in the primer and NJ bullet remained consistent through decomposition and were used to discriminate NJ and FJ samples based on differences in average element ratios.

This study proved ICP-OES to be successful in detecting elements present in GSR in fresh tissue, while only moderately adequate in detection over a period of decomposition. ICP-MS was more sensitive for the elements of interest and demonstrated the persistence of GSR over time, whereas ICP-OES was less successful in detecting all of the elements of interest

especially in FJ samples. The high Pb concentrations did allow for the differentiation of bullet type and firing distance in the fresh and decomposition studies using ICP-OES. A more rigorous optimization of the ICP-OES specifically for the elements of interest and fresh standards would improve the overall results; however, the inherent low sensitivity for Sb may not be overcome without the use of more sensitive analytical instrumentation.

The biological processes of decomposition and environmental conditions were an impedance in visually observing GSR on porcine tissue and in some instances identifying the gunshot wounds. Despite these problems, elements commonly associated with GSR were detected on tissue after 26 days decomposition using ICP-OES (NJ samples only) and ICP-MS. ICP-OES proved to be an effective technique that would be capable of routine analysis of GSR on fresh tissue in a forensic science laboratory. In cases of decomposition, a more sensitive technique, such as ICP-MS would be the most practical choice to identify GSR.

5.2 Future Directions

This study showed both the utility and limitations of ICP-OES in the analysis of elemental composition of GSR and leaves opportunity for further research. One limitation of this study was the wide concentration range of standards required to accommodate the extreme concentration differences in fresh tissue and tissue samples collected at the end of decomposition. In this study, high concentrations of Pb were deposited in NJ samples and required dilutions of all microwave digests prior to instrumental analysis to maintain consistent experimental conditions. A study conducted on firing distance discrimination solely using FJ ammunition or ammunition with a lower lead content would provide for a better assessment of the capability of ICP-OES by narrowing the standard calibration range and giving greater confidence to quantitation.

As a consequence of the levels of iron (Fe) and zinc (Zn) found in the control tissue, the element concentrations were excluded from further discussion in this study. These elements are commonly found as minor or trace components in GSR, but are also present in blood and skin tissue. One way in which bulk analysis techniques, such as ICP-OES, suffer is that they detect all elements in a solution and are not specific to GSR particles like scanning electron microscopy with energy dispersive X-ray spectroscopy (SEM/EDS). In order to overcome the problem of specificity in tissue analysis, a full elemental profile of control tissue needs to be obtained so that elements common to GSR can be identified and quantified prior to GSR analysis. Once a baseline of element concentrations in tissue is obtained, the elemental concentrations in GSR tissue samples can be viewed with greater confidence.

In the guide for GSR particle analysis, SWGGSR lists major, minor, and trace components that are commonly identified by EDS and outlines criteria for reporting. The terms major, minor, and trace are not strictly defined, but their application to an element is based on peak height of that element relative to the highest peak in the EDS spectrum. ICP-OES and ICP-MS are both suitable methods to identify the elemental components of GSR from a variety of sources due to their low limits of detection and wide linear ranges and could be used to create standardized thresholds for defining major, minor, and trace components that would be analogous to those for SEM/EDS.

In this study, Pb and Sb were both found useful in the differentiation of bullet type; however, these two elements are no longer as prevalent in primer formulations as they were in the past. Lead compounds are now being excluded from primers due to the toxicity of lead, while some primer formulations contain Pb and omit either Sb or Ba compounds. The absence of one or more of the three characteristic compounds could lead to ambiguity in GSR

identification. ICP-MS is a very sensitive instrument that would be very effective in detecting the low level components in primers from different manufacturers, such as cobalt, zirconium, and strontium that could be used to positively identify GSR.